# Hitless Defragmentation to Increase Traffic Admissibility in Elastic Optical Networks

Seydou Ba

Department of Communication Engineering and Informatics

The University of Electro-Communications

A thesis submitted for the degree of

*Doctor of Philosophy*

March 2017

**APPROVED BY SUPERVISORY COMMITTEE:**

**Chairperson:** Prof. Eiji Oki

**Member:** Prof. Naoto Kishi

**Member:** Prof. Yasushi Yamao

**Member:** Prof. Hiro Ito

**Member:** Prof. Motoharu Matsuura

Date of the final-defense: 2017/02/08

# 概要

エラスティック光ネットワークにおいて、スペクトルフラグメンテーションはスペクトル資源の有効利用の障害となる。エラスティック光ネットワークにおけるスペクトルフラグメンテーションを解消するためのデフラグメンテーション方法の多くの研究がなされている。論文中のデフラグメンテーション方法の中で、ヒットレスデフラグメンテーションはトラヒックの中断無しでフラグメンテーションを解消するアプローチとして紹介されている。それは、終了した光パススペクトルの空きを埋めるように既存のスペクトルを整調するので、新たな光パス要求の許容を促進する。

しかし、ヒットレスデフラグメンテーションはこれまで使われてきているファーストフィット割り当てで段階的に整調するという制約がある。ファーストフィット割り当てはスペクトルを下の方へと詰める。これは整調される必要がある沢山の光パスをもたらし、それぞれの光パスが他の整調を妨げるという条件を持つ。本論文は、エラスティック光ネットワークにおける許容トラヒック量を増加させるための、ヒットレスデフラグメンテーションに基づく 2 つの方式を提案する。

最初に、デフォルトのエラスティック光ネットワークにおけるヒットレスデフラグメンテーションのための経路分割方式を提案する。提案方式は光パス間の整調の妨げを避けることにより整調の可能性を増加するためにファーストラストフィット割り当てで経路分割を利用する方式である。ファーストラストフィット割り当ては、一つはファーストフィット、もう一つはラストフィットで割り当てる 2 分割にして用いられる。異なる分割に割り当てられる光パスは他の光パスを妨げることはない。したがって、経路分割は整調の際に光パス間の妨げを避ける。経路分割問題は全体の妨げを最小化する最適化問題として定義される。

2 つ目に、1+1 パスプロテクションにおける、パス切り替えを用いたデフラグメンテーション方式を提案する。従来のデフラグメンテーションアプローチは定められた主要パスと予備パスを想定している。これは、主要パスによるフラグメンテーションを引き起こし、ヒットレスデフラグメンテーションを達成する際に障害となる。提案方式は、1+1 プロテクションにおける主要パスと予備パスを同時に切り替えるという方式である。これにより両方の光パスの再割り当てを許し、予備パスが機能している間もヒットレスデフラグメンテーションを行うことができる。パスの切り替えを考える上で、パスの切り替えと再割り当て操作の回数を制限しつつ、スペクトルフラグメンテーションを最小化する、静的なスペクトル再割り当ての最適化問題として定義する。

それぞれの提案方式に対して、最適化問題として定義した後、整数線形計画問題として定式化する。そして、定義した問題が NP 完全であることを証明する。整数線形計画問題では扱いにくい問題であることを示し、大規模ネットワークを用いてヒューリスティックアルゴリズムを紹介する。性能評価により、提案方式は従来方式よりも全体の許容トラヒック量を増加させることを示す。

# Abstract

In elastic optical networks (EONs), a major obstacle to using the spectrum resources efficiently is spectrum fragmentation. Much of the research activities in EONs focuses on finding defragmentation methods which remove the spectrum fragmentation. Among the defragmentation methods presented in the literature, hitless defragmentation has been introduced as an approach to limit the spectrum fragmentation in elastic optical networks without traffic disruption. It facilitates the accommodation of new request by creating large spectrum blocks, as it moves active lightpaths (retuning) to fill in gaps left in the spectrum by expired ones.

Nevertheless, hitless defragmentation witnesses limitations for gradual retuning with the conventionally used first fit allocation. The first fit allocation stacks all lightpaths to the lower end of the spectrum. This leads to a large number of lightpaths that need to be retuned and are subject to interfere with each other's retuning. This thesis presents two schemes, which are based on hitless defragmentation, to increase the admissible traffic in EONs.

Firstly, a route partitioning scheme for hitless defragmentation in default EONs is presented. The proposed scheme uses route partitioning with the first-last fit allocation to increase the possibilities of lightpath retuning by avoiding the retuning interference among lightpaths. The first-last fit allocation is used to set a bipartition with one partition allocated with the first fit and the second with the last fit. Lightpaths that are allocated on different partitions cannot interfere with each other. Thus the route partitioning avoids the interferences among lightpaths when retuning. The route partitioning problem is

defined as an optimization problem to minimize the total interferences.

Secondly, this thesis presents a defragmentation scheme using path exchanging in 1+1 path protected EONs. For 1+1 path protection, conventional defragmentation approaches consider designated primary and backup paths. This exposes the spectrum to fragmentations induced by the primary lightpaths, which are not to be disturbed in order to achieve hitless defragmentation. The presented path exchanging scheme exchanges the path function of the 1+1 protection with the primary toggling to the backup state while the backup becomes the primary. This allows both lightpaths to be reallocated during the defragmentation process while they work as backup, offering hitless defragmentation. Considering path exchanging, a static spectrum reallocation optimization problem that minimizes the spectrum fragmentation while limiting the number of path exchanging and reallocation operations is defined.

For each of the presented schemes, after the problem is defined as an optimization problem, it is then formulated as an integer linear programming problem (ILP). A decision version of each defined problem is proven NP-complete. A heuristic algorithm is then introduced for large networks, where the ILP used to represent the problem is not tractable. The simulation results show that the proposed schemes outperform the conventional ones and improve the total admissible traffic.

*To my parents*

# Acknowledgements

This thesis is the summary of my doctoral study at the University of Electro-Communications, Tokyo, Japan. I am grateful to a large number of people who have helped me to accomplish this work.

First of all, I would like to express my sincere gratitude to my advisor, Professor Eiji Oki, for his mentorship, guidance and encouragements. By working under the supervision of Professor Oki, I received an invaluable experience that helped me to shape my academic and professional skills. Second, I would like to thank Professor Naoto Kishi for his encouragements and constant support since I came to Japan.

I would also like to thank Professor Yasushi Yamao, Professor Hiro Ito and Professor Motoharu Matsuura for being part of my judging committee and providing their precious comments to improve my thesis.

I would like to thank Dr. Bijoy Chand Chatterjee for his valuable comments for my research.

I would like to thank my Japanese language teachers at the University of Electro-Communications, the personnel of the Center for International Programs and Exchange, the International Student Office, and the Musashino International Friendship Organization for their precious support during my stay in Japan.

Finally, I want to deeply thank my family for all their love and support. Also thank for kindness help for all of my friends.

# Contents

# List of Figures

# List of Tables

# Chapter 1

# Introduction

The traffic volume in communication networks witnesses a continuous growth due to the increasing number of connection demands and higher capacity requirements. This trend becomes more and more highlighted every passing year with the widespread of high-definition television, 3-dimensional video-on-demand, e-learning, and cloud computing. As the volume of traffics and their capacity requirement rapidly increase, much focus is being put in researches to find efficient ways to use the available network resources.

The elastic optical network (EON) [1, 2, 3, 4] has been introduced to relieve the international telecommunication union telecommunication standardization sector (ITU-T) rigid frequency grid. The latter has already reached its limits for traffic above 100Gb/s. EONs offer a flexible and elastic frequency allocation as only the needed bandwidth for a given traffic demand is allocated. Due to its flexibility, EONs provide new features in terms of segmentation and aggregation of spectral resources (sub-wavelength and super-wavelength), efficient accommodation of multiple data rates, as well as elastic variation of allocated resources [3].

## 1.1 Elastic optical networks

EONs have been introduced to address the issues of the existing scalable networks by providing spectrum-efficient and scalable transport of 100 Gb/s services and beyond. This is achieved through the introduction of flexible granular grooming in the optical frequency domain.

Due to its flexibility, EONs provides new features in terms of segmentation and aggregation of spectral resources (Sub-wavelength and Super-wavelength), efficient accommodation of multiple data rates, as well as elastic variation of allocated resources. The unique features of EON are illustrated in Fig. 1.

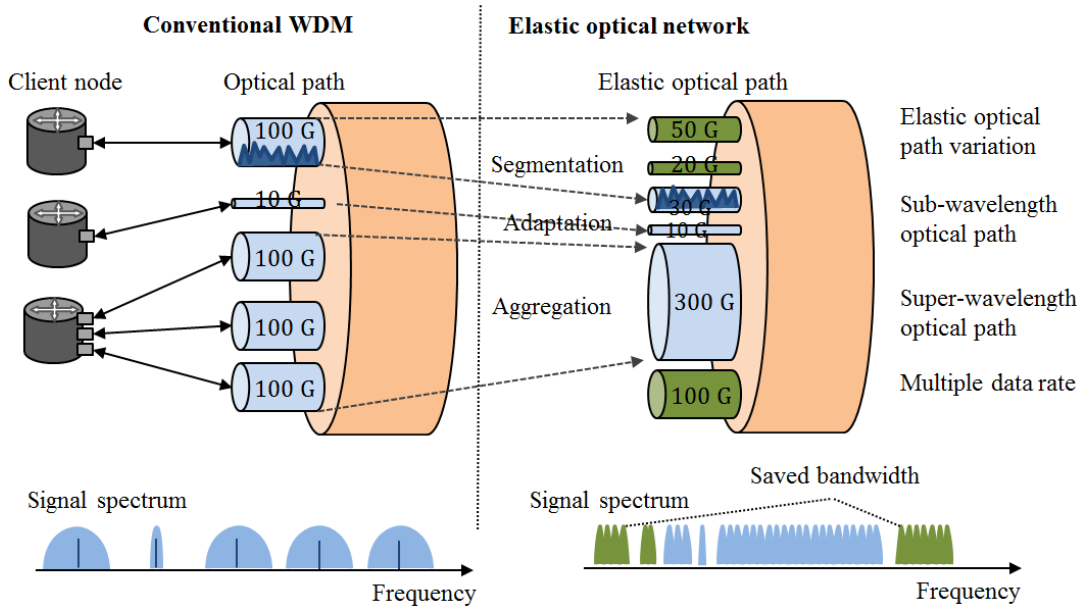


**Figure 1.1:** Comparison on Bandwidth utilization between EONs and the ITU-T fixed grid network

### 1.1.1 Enabling technology

Advances in optical transmission techniques and devices have favored the emergence of EONs [5, 6]. The introduction of advanced modulation formats and wavelength cross-connects (WXCs) enable carrying the growing traffic volume over long-haul distances without optical-electrical-optical (OEO) conversion [7]. The paths with bandwidths determined by the volume of client traffic are allocated through rate-flexible transponders from the transmitter and send through bandwidth-variable (BV) wavelength cross-connects (WXCs) to the receiver [5].

#### 1.1.1.1 Spectrally efficient superchannel

There are two common schemes used in rate-flexible transponders to achieve a spectrum efficient modulation for super-channel transmitter [8]. The first scheme is based on optical orthogonal frequency-division multiplexing (OFDM) [9, 10, 11]. A frequency-locked multicarrier generator is utilized to generate equally spaced subcarriers. The generated subcarriers are first separated by a wavelength-division demultiplexer (DMUX), then individually modulated with parallel modulators, and finally coupled to generate a spectrally overlapped superchannel.

The second scheme is based on wavelength division multiplexing (WDM) of subchannels which have an almost rectangular spectrum with a bandwidth close to the Nyquist limit for intersymbol-interference-free transmission [12, 13]. The subchannels are aligned with the frequency spacing close to the baud rate, which is the Nyquist limit, while avoiding inter-subchannel spectral overlap. This scheme is referred to as Nyquist-WDM [8].

#### 1.1.1.2 Optical transponders

Three models of transponder can be found [14], namely mixed-line-rate (MLR) model, multi-flow (MF) model, and bandwidth-variable (BV) model. The MLR model employs a few types of transponders, each with a different bit rate, for example 40, 100 and 400 Gb/s transponders to suit a wide range of traffic demands. The MF model uses a MF transponder with several sub-transceivers, than can be allocated to different demands, each of which has a fixed bitrate capacity. The BV model supports all types of traffic demands with a single BV transponder, which assigns the fewest possible spectral resources to support traffic demands with a 400 Gb/s maximum bit-rate.

As shown in the study presented in [14], the BV model offer better spectrum efficiency and the lowest port consumption rate. Also it is more suited for energy reduction purpose owing to the reduced active resource due to the use of sub-transceivers. A next generation optical transponders (S-BVT) has been investigated in [15]. The authors provided a design architecture and considered several transmission techniques to build the transponder.

#### 1.1.1.3 Bandwidth-variable wavelength cross-connects

Optical nodes with BV switching elements, which are EON compliant, can be realized by wavelength-selective switches (WSSs) based on Liquid Crystal on Silicon (LCOS) technology [16, 17, 18]. A WSS is a 1xN switch or filter providing continuously-tunable and variable seamless transmission spectrum. In a bandwidth-variable WSS, the incoming optical signals with differing optical bandwidths and center frequencies can be routed to any of the output fibers. These technologies allow us to allocate the required bandwidth in nodes along the optical path [19].

In [20] the switchless elastic rate node (SERANO) block is positioned as compliment to WSSs. It integrates transmission and data-forwarding in EONs without electronic switch with packet-level processing. SERANO aim to provide on-the-fly adaptation functions such as 3R regeneration or modulation format change.

### 1.1.2 Routing and spectrum allocation

The routing and spectrum allocation (RSA) problem [21, 22, 23, 24, 25] is considered one of the key functionalities in EONs. It is, given a set of traffic demands, the problem of setting up lightpaths by routing and allocating the necessary spectrum (required sub-wavelengths) to each traffic demand. In EONs, a spectrum lightpath is an all-optical trail established between the source and destination nodes by using one or multiple consecutive sub-wavelength.

The RSA is performed under several constraints [21]. They are the traffic demand constraint, the sub-wavelength consecutiveness constraint, spectrum continuity constraint, the carrier capacity constraint, and the guard band constraint. The traffic constraint requires all the traffic to be routed from source to destination. The carrier capacity and the guard band constraints ensure that, on each link, a sub-carrier is allocated to at most one demand at the time and that two sub-carriers do not overlap. The sub-wavelength consecutiveness and spectrum continuity constraints differentiate the RSA problem to the routing and wavelength assignment (RWA) problem in wavelength division multiplexing (WDM) networks. They ensure that, with the flexible spectrum allocation in

EONs, the lightpath allocated to a demand is of the requested size and consists of consecutive sub-wavelengths (slot block) that are available through its routing path.

### 1.1.3 Impairment aware adaptive modulation

Distance adaptive modulation has been vastly investigated alongside RSA allocation in EONs [26, 27]. With EONs, the modulation level define the spectrum needed to convey a given bit-rate demand. For example, if $f$ GHz is needed to transmit a signal with a BPSK modulation, $f/n$ GHz would be enough to transmit that signal with a $2^n$-PSK modulation. However, the distance for which the signal can be transmitted with an acceptable quality of transmission is inversely proportional. A more spectrum efficient modulation can only be transmitted over a shorter distance. Therefore, depending on the required quality of transmission, the modulation level can be adapted in order to reduce the spectrum usage.

In [26] the authors propose a method of adaptive optical spectrum allocation in EONs where the bandwidth is optimized to balance transmission distance and signal filtering penalty. In [28], authors describe the concept and enabling technology for an elastic optical transponder and regenerator that create and regenerate multiple optical flows with various bit rates and modulation formats. They scheme, if applied, leads toward energy and spectrum efficient optical transport networks.

Impairment awareness and optical regeneration in EON have been investigated in [29, 30]. Authors study the impairment-aware dynamic routing and subcarrier allocation problem in translucent SLICE networks. They proposed an impairment-aware routing algorithm that tries to balance traffic flows evenly across the network to reduce respectively the blocking probability and improve the OSNR.

In [31], the problem of regenerators' placement in translucent EONs has been investigated. Author evaluated the effect of 3R-regeneration on the spectral efficiency (SE) and showed that by employing regenerators the spectrum usage of translucent EON is considerably reduced.

## 1.2 Related works on spectrum defragmentation

One of the major concerns in EONs is the spectrum fragmentation induced by the dynamic allocation and tearing down of connections with variable size [32, 33]. When larger connections are replaced by smaller ones, spectrum gaps are left, and this increases the possibility for new connections to be rejected due to the spectrum consecutiveness and continuity constraint of the RSA problem. In literature, several defragmentation methods have been presented to limit the fragmentation effect and reduce the network bandwidth blocking probability. The bandwidth blocking probability (BBP) is defined as a ratio of the number of blocked connection requests to the number of connection requests in the network. The following subsections present the related works on defragmentation schemes with or without considering hitless.

### 1.2.1 Non-hitless defragmentation schemes

W. Shi et al. studied [32] the theoretical effect of bandwidth fragmentation on blocking probability in EONs in order to reduce the BBP. Their results indicate that the available slot blocks' (SB) alignment over links and the size of the SBs are critical to the assignment of new demands. Taking this direction, Y. Yin et al. considered this issue in [34] and formulated the fragmentation as two-dimensional problem, such as (i) fragmentation problem, and (ii) misalignment problem. They presented proactive fragmentation-aware algorithms to prevent blocking of incoming lightpath requests. The algorithms are presented as routing and spectrum allocation schemes, which aim to fragment the least number of continuous spectral blocks on candidate links, while filling up as many misaligned spectral slots as possible on neighbouring links. One of the proposed algorithms also includes congestion avoidance to limit request blocking due to network congestion when the network is heavily loaded. In [35], the authors presented a fragmentation-aware RSA scheme based on the distribution of traffic bandwidth. They advocate the use of several different schemes for each step of the RSA process to increase the RSA efficiency and reduce computational complexity.

In [36], R. Wang et al. have shown that the lightpath provisioning efficiency is improved by using dedicated partitions for different bandwidth lightpaths in

dynamic EONs. They studied three spectrum management methods, namely, (i) complete sharing with partitioning, (ii) pseudo partitioning, where the connections with high and low bandwidth requests are respectively allocated lightpaths at the high and low ends of the spectrum, and (iii) dedicated partitioning, where each partition of spectrum carries uniform data rate and where they seek for an optimal partitioning. A similar approach was presented in [37, 38] as the authors use subcarrier-slot partition in order to promote both slot blocks alignment and spectrum consecutiveness. They use the first-last fit allocation and assign lightpaths to the partitions based on the links utilized by particular connections.

M. Zhang et al. in [39, 40] presented a study on the defragmentation process. They considered the questions of "when, what and how to defragment?". The joint answer to these questions leads them to algorithms, which accomplish defragmentation through proactive network reconfiguration with little rerouting and minimum traffic disruption. They employ connections selection strategies, defragmentation based RSA, and dependency graphs to perform rerouting with best-effort traffic migration and minimum traffic disruption. Additionally, they studied in [40] the effect of the relation between the initial routing algorithm and the rerouting algorithm. They also added an adaptive defragmentation timing selection policy.

The above mentioned defragmentation methods are either proactive with no reactive measure to additional fragmentation induced by expired connection or cause traffic disruption when they are reactive. X. Chen et al. introduced in [41] a multi-path defragmentation instead of applying proactive solutions or reactively rearranging the spectrum. They use traffic splitting to aggregate spectrum fragments. In [42], the authors explored the split spectrum approach (SSA) and presented mechanisms to attack the problem. However, this method challenges some of the RSA problem constraints, such as the spectrum consecutiveness and presents path differential delay consideration. In [43], the author proposed an EON node with defragmentation functionality implemented with SDN control. They claim to avoid fragmentation by slicing a bulk traffic and fitting different parts into different spectrum fragments at intermediate nodes.

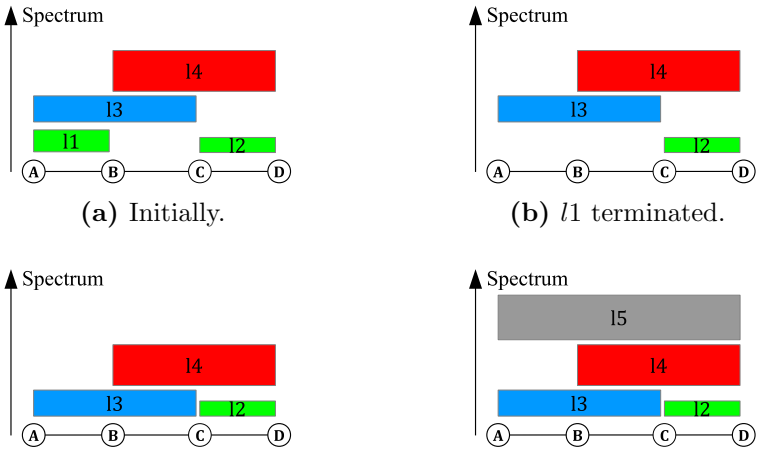


**(a)** Initially.

**(b)** $l1$ terminated.

**(c)** Hitless defragmentation.

**(d)** $l5$ added.

**Figure 1.2:** Example of hitless defragmentation.

### 1.2.2 Hitless defragmentation schemes

Hitless defragmentation has been presented as a defragmentation method that works continuously in EONs without service disruption [44]. It advocates retuning the spectrum of the already established lightpaths after a connection is terminated to fill in the gap left behind. This process is executed without re-routing, and therefore it does not require any traffic interruption. Figure 1.2 shows an example of hitless defragmentation, where the horizontal axis indicates the routing paths and the vertical axis indicates the spectrum. In this example, we use five signals, such as, $l1$ (200 Gbps between $A - B$), $l2$ (100 Gbps between $C - D$), $l3$ (100 Gbps between $A - C$), $l4$ (400 Gbps between $B - D$), $l5$ (200 Gbps between $A - D$). Initially signals $l1$ to $l4$ are active. Then $l1$ is terminated. Hitless defragmentation is applied to move down $l3$ and $l4$. Eventually $l5$ is added.

Two retuning approaches, namely, (i) hop-retuning [45], and (ii) push-pull retuning [46] have been demonstrated in the literature for hitless defragmentation, which are presented in the following.

#### 1.2.2.1 Hop retuning

Hop retuning allows the retuning of a lightpath to any available spectrum slot regardless of whether it is contiguous or not. Its enabling technology was introduced in [45]. The authors use fast tunable lasers at the transmitter and burst-mode coherent receivers with fast wavelength tracking at the receiver. The fast auto-tracking technique involves an athermal arrayed waveguide grating (AWG) with a detector array sensing a change in the transmission wavelength (fig 1.3).

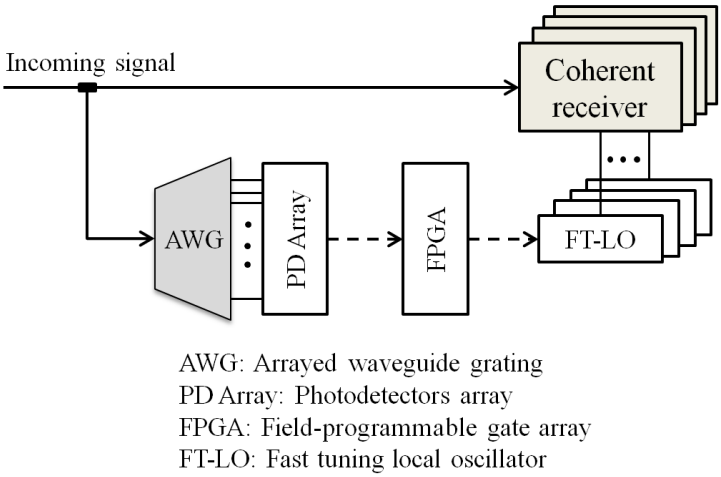


**Figure 1.3:** Illustration of wavelength tracking at coherent receiver using AWG, FPGA, PD array, and FT-LO.

M. Zhang et al. [47] presented two hitless defragmentation algorithms; to maximize the spectrum rejoins (MSR) and to minimize the number of operations (MMO), respectively. The MSR algorithm is applied in both hop retuning and spectrum sweeping (push and pull) while the MMO is used for hop tuning only. Their results indicate that both algorithms reduce the BBP compared to the spectrum sweeping technique.

However, as stated in [45], hop retuning technology is not simple to be deployed in case of a fine granular grid. This is due to the sensitivity of the spectrum wavelength detection. With each fast tuning laser/coherent receiver couple covering only the range of a spectrum slot, the number of photodetectors needed is equal to the number of spectrum slots. As an example, in a 12.5 GHz grid, a 400

port AWG and 400 photodetectors are required, this increases the system complexity. Therefore, hop retuning technology is not preferred as a defragmentation approach for fine granular grid.

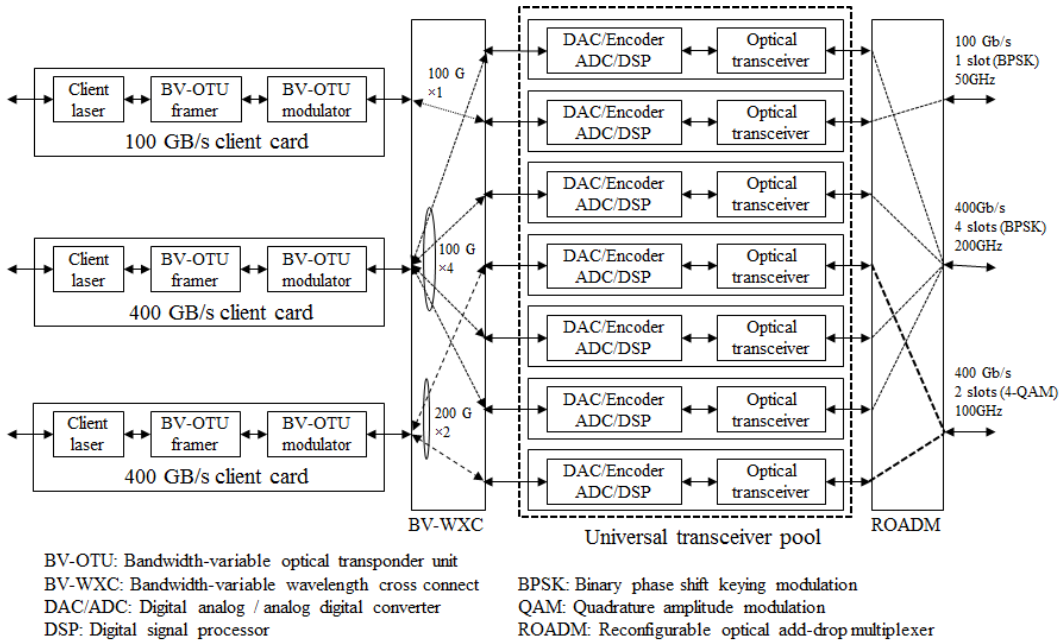


**Figure 1.4:** Node architecture using universal transponders

#### 1.2.2.2 Push-pull retuning

The technology demonstrated in [46] for a push and pull approach is used for all spectrum grid range. The authors introduced a dynamic and flexible network node architecture using modulation flexible universal transceivers (fig 1.4). The authors of [48] also demonstrated a push pull defragmentation technique. Their technique is based on dynamic lightpath frequency retuning upon proper reconfiguration of allocated spectrum resources. The retuning is executed gradually and the spectrum change cannot be jumped. It is performed by all involved device in a coordinated manner under distributed control environment or a centralized network controller. This process is executed without re-routing and therefore does not require any traffic interruption (fig 1.5). Other experiment demonstrations

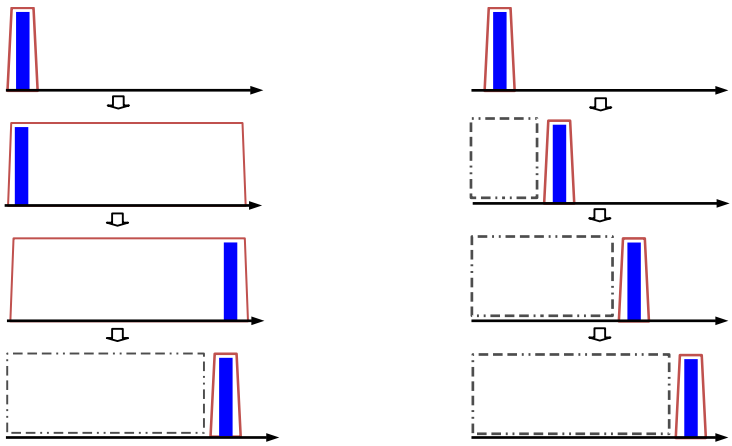

**(a)** Sequential BV-WSS control

**(b)** Synchronous BV-WSS control

**Figure 1.5:** Push pull retuning.

of hitless defragmentation have been conducted [49, 50]. However, to the best of our knowledge, the demonstrations have been limited to test-beds, and the impairment related to the transmission distance have not been considered.

Figure 1.5 illustrates the BV-WSS control during the retuning process. There are two types of control, namely sequential BV-WSS control (see Fig. 1.5(a)) and synchronous BV-WSS control (see Fig. 1.5(b)). They are differentiated by how they approach the retuning process, sequential BV-WSS control uses one large step retuning during which the spectrum between the source and destination bandwidth are not available while synchronous BV-WSS control proceeds by successive small steps retuning and after each step, available spectrum can be used. Sequential BV-WSS control is simpler and can be used without causing request blocking when the retuning time is small compared to the request average inter arrival time. However if retuning time is not small enough, using synchronous BV-WSS control maybe preferable.

The retuning time in push pull retuning is determined considering a retuning step width of 2.5 GHz and sweeping rates of 1, 10, 100, or 1000 ms/step [46]. For an example, in a 12.5 GHz granular EON, 5 ms per slot block are needed at each step for a sweeping rate of 1 ms/step (respectively 0.5 s for 100 ms/step).

The self-optimizing defragmentation method also presented in [46] is further explored in [51] with considerations, such as distance adaptive modulation.

In [52], the authors presented a hitless optical path shift (HOPS) approach using push and pull retuning. Initially, they considered a proactive defragmentation that maintains the spectrum to a delta state where no lightpath is reallocated. Their proposed algorithm is triggered when a lightpath leaves. Considering that frequent defragmentation upon each lightpath termination is undesirable, they introduced a reactive defragmentation. With the reactive approach, a defragmentation is executed only when necessary, namely when a connection cannot be established without defragmentation. Also, only relevant lightpaths are defragmented to accommodate the incoming request to avoid lightpaths provisioning delay.

### 1.2.3 Hitless defragmentation on protected networks

Link failures present another challenge for EONs. Optical networks carry huge amount of information (in the order of Tb/s) and any interruption of the data flow leads to massive data loss. Since optical fibres are subject to impairments, such as being cut, providing network with protection is imperative. This has motivated a continuous research effort to offer protection against failures and provide network resiliency. Several techniques have been considered [53, 54]. They range from, and not exhaustively, span restoration, p-Cycles, 1+1/1:1 end-to-end path protection, and shared backup path protection (SBPP). These techniques were developed in traditional wavelength division multiplexing (WDM) networks and are being extended to EONs. Protection techniques are mainly divided into shared protection and dedicated protection techniques.

Shared protection techniques reduce the spectrum resource used for protection. In [55] two hitless-defragmentation algorithm have been proposed for SBPP, namely by sequentially releasing and re-establishing protection lightpaths, and by jointly releasing and re-establishing protection lightpaths. In [56], the authors considered span restoration in elastic optical networks. They develop integer linear programming (ILP) models to minimize both required spare capacity and

maximum used spectrum slots index under different spectrum conversion capabilities. They considered i) no spectrum conversion, ii) partial spectrum conversion, and iii) full spectrum conversion. The authors of [57] considered the p-cycle protection technique, which provides ring-type protection and the speed of restoration of meshes. Similar to [56], they aimed to minimize required spare capacity and the maximum used spectrum slots index and formulated an ILP. Both works in [56] and [57] also apply the bandwidth squeezed restoration (BSR) technique [58]. In [59], the authors presented algorithms that provide path protection using p-cycle paths. They claim 100% protection against single and double link failures.

The works in [60, 61] used SBPP in EONs. SBPP proactively reserves backup paths that are independent of the primary paths. When a failure occurs, the signal is recovered from the protection path regardless of where the failure occurs. The authors focus on providing maximally shared capacity on the backup paths for static traffic demand. They present heuristic algorithms in both works. An ILP model is also formulated in [61] for optimal sharing. For dynamic traffic, SBPP in EONs has been presented [62, 63]. The authors of [62] advocate the use of an algorithm applying different strategies for primary and backup resources using first-fit for primary paths and a modified last-fit for backup paths. They aim to reduce the fragmentation and to increase the shareability. In [62], the author evaluated conservative and aggressive backup sharing policies. The sharing policy is considered as aggressive when it only requires the corresponding working lightpaths to be link-disjoint. It is considered as conservative when in addition to the working lightpaths being disjoint, the sharing lightpaths must have the same bandwidth.

Dedicated protection techniques offer resistance against multiple link failures and allow for instantaneous recovery. In [64], dedicated path protection (DPP) has been considered with static traffic demands. The authors focused on the RSA problem and formulated an evolutionary algorithm to search for optimal solutions. In [65], the authors presented a 1+1 path protection defragmentation approach in dynamic EONs. Their focus is set on the defragmentation advantage offered by the backup paths. They consider that, since the backup paths by nature are used only in case of failure on their corresponding primary path, they can be reallocated and/or rerouted for defragmentation purpose without causing

any traffic disruption. Therefore, the authors achieve hitless defragmentation by performing spectrum defragmentation on them.

A survey on the state of the art of survivable EONs is presented in [53]. The authors first review the literature around aspects, such as, spectrum resource sharing among backup lightpaths, and sharing of high-speed optical transponders. Then they discuss the ongoing research issues and future challenges, spectrum defragmentation on path-based protection among others.

To deploy hitless defragmentation in 1+1 path protected EONs, one can apply the approach presented in [65]. Yet, that may not be enough to eliminate fragmentation since it focuses on defragmenting only the backup paths; the fragmentations caused by primary lightpaths are overlooked. To overcome this issue, and without causing traffic disruption, hitless defragmentation is to be applied on working primary paths too. Researches have been presented for hitless defragmentation on working lightpaths using spectrum retuning [51]. With spectrum retuning, the allocated bandwidth of a working lightpath is swept from its initial position to a new one, while the signal is still being transmitted, to fill in gaps left in the spectrum. Spectrum retuning is therefore a candidate for complementary defragmentation by retuning the primary paths when the approach presented in [65] is used.

Despite applying hitless defragmentation on primary lightpath, we still face the end-of-line phenomenon with spectrum retuning. When spectrum jump is not allowed, the retuning is done gradually and it is subject to the interferences of other lightpaths that share a link with the lightpath being retuned. An end-of-line situation occurs when the retuning process is stopped (if started) due to those interferences. Thus, even when spectrum retuning is applied on primary lightpaths, the scheme presented in [65] is subject to fragmentations caused by primary lightpaths.

## 1.3 Problem statement

### 1.3.1 Requirements

Spectrum defragmentation reduces the bandwidth blocking probability in EONs. In other words, it increases the possibility to add more traffic by avoiding the rejection of incoming lightpath requests due to the spectrum fragmentation. However this can be done to the expense of the networks quality of service as it may causes traffic disruption. In this work we intend to apply spectrum defragmentation without any traffic disruption. Also the approach has to be tractable at the actual spectrum range of EONs.

### 1.3.2 Issues to be addressed

Several works have been presented to limit the fragmentation issue in EONs. Mostly, defragmentation schemes aim to promote slot block alignment and spectrum consecutiveness. Taking that direction, Hitless defragmentation retunes the spectrum slots in order to fill in emptied slot blocks without interrupting established traffics. It presents a viable option to avoid traffic disruption. Hitless defragmentation can be deployed with push-pull retuning for all spectrum grid range.

However, with hitless defragmentation, when spectrum jump is not allowed, end-of-line situations may occur. An end-of-line situation is defined by a situation where a lightpath cannot be retuned to fill in a gap left by expired connection due to the interference of another lightpath preventing it from being moved further. When an end-of-line situation occurs, the retuning of a lightpath, if started, is stopped.

Figure 1.6 is an illustration of an end-of-line situation. In this example, there are initially four lightpaths $l1$, $l2$, $l3$, $l4$ and the min-hop routing leads to the use of routes $A$-$B$-$D$ and $A$-$B$-$E$ for demands from node $A$ to nodes $D$ and $E$, respectively (see Fig. 1.6(b)). When $l1$ is removed (see Fig. 1.6(c)), its emptied slot could be refilled by already established connection(s) ($l3$). However, in this case, it cannot be retuned with hitless defragmentation without spectrum jump;

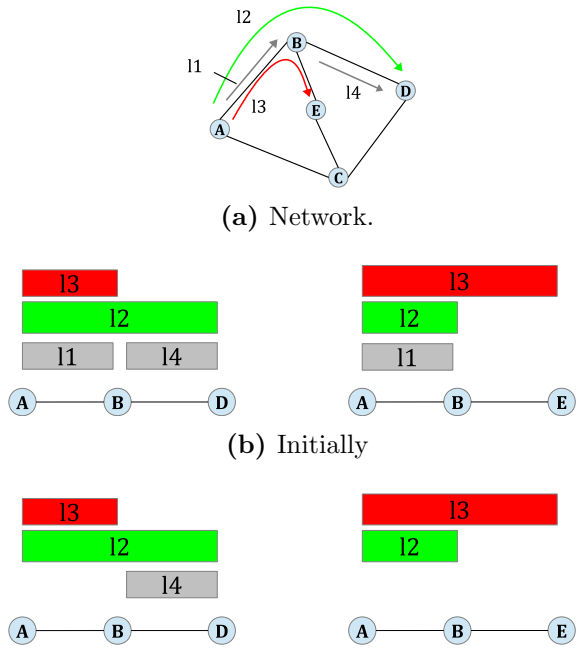


**(a)** Network.

**(b)** Initially

**(c)** No retuning possibility after $l1$ terminated.

**Figure 1.6:** Links state on routes A-B-D and A-B-E.

$l3$ (route $A$-$B$-$E$) cannot be retuned before $l2$ (route $A$-$B$-$D$), as $l3$ shares link $AB$ with $l2$.

Hitless defragmentation based schemes conventionally are implemented using the first-fit allocation policy, where incoming requests are allocated to the lowest available spectrum slots. While this has the advantage of simplicity, it is exposed to the end-of-line situations. With all lightpaths stacked one over the other, it is likely to have the retuning of a lightpath blocked by the interference of another one. This restrains the possibility of retuning.

A similar effect is observed when several retuning operations are required after a connection expires. A retuning operation correspond to the action of moving one lightpath from an initial spectrum index to another index. Multiple retuning operations may be required after a connection expires. When a lightpath is removed, the next movable lightpath is retuned to fill in the gap left behind, thus creating new space. In turn, other lightpath(s) may need retuning to fill in for the retuned lightpath(s). As a result, the retuning after an expired lightpath

takes time and new added lightpaths between retuning operations lead to more end-of-line situations, particularly when the retuning speed is not high enough.

While hitless defragmentation offers spectrum defragmentation without traffic disruption, its effectiveness is limited by end-of-line situation when the first-fit allocation policy is used. Therefore the challenge of this work is to define a hitless defragmentation scheme to maximize the admissible traffic by avoiding end-of-line situations without spectrum jump.

Note that, for the remaining of this paper, we refer to the push-pull hitless defragmentation method as the hitless defragmentation.

## 1.4 Contributions

This thesis presents hitless defragmentation schemes that allows increased traffic load admissibility, as well as reliability in EONs. We advocate the use of efficient defragmentation methods that do not cause any traffic disruption. First, we propose the route partitioning scheme to tackle the fragmentation in EONs. Then, we consider 1+1 protected EONs, and propose the path exchanging scheme.

The proposed route partitioning scheme uses the first-last fit allocation with the route partitioning to further the possibilities of lightpath retuning by avoiding retuning interference among connections. A retuning interference occurs when a lightpath could not be moved to its intended index without jumping part of the spectrum. This is due to lightpath enabled to be gradually moved only as far as to the next spectrum index being used on one of its links. To be able to gradually retune a lightpath whenever it is possible without recurring to spectrum jump, the first-last fit allocation is used. It offers more options than the first fit allocation. In particular, the route partitioning used as a side selection policy reduces the retuning time and limits lightpath interferences.

In 1+1 path protected EONs, we propose a defragmentation scheme that allows exchanging the primary and backup paths' function of a 1+1 protected path. Conventional defragmentation approaches consider designated primary and backup paths. This exposes the spectrum to fragmentations induced by the primary lightpaths, which are not to be disturbed in order to achieve hitless

defragmentation. By allowing the path exchanging function, lightpaths are toggled from being primary paths to become backup paths while the corresponding backups are toggled to become primary paths. This allows both lightpaths to be reallocated during the defragmentation process while they work as backup, offering hitless defragmentation with no additional network component.

For both considered scenarios, we define the problem as an optimization problem. We then formulate the problem as an integer linear programming problem (ILP). We prove that a decision version of the defined problem is NP-complete. We introduce a heuristic algorithm for large networks, where the ILP used to represent the optimization problem is not tractable. The simulation results show that the proposed schemes outperform the conventional ones and improve the total admissible traffic.

## 1.5 Organization of thesis

The organization of the thesis is shown in Fig. 1.7. The thesis consists of six chapters. The route partitioning scheme is considered in Chapters 2 and 3. The path exchanging scheme is considered in Chapters 4 and 5. Chapter 6 concludes the thesis.

Chapter 2 introduces the route partitioning scheme and its mathematical formulation. The limits of hitless defragmentation using the first fit are described before defining the route partitioning scheme. The route partitioning problem is formulated into an ILP and proven to be NP-complete.

A heuristic for the route partitioning scheme is developed in Chapter 3. The heuristic algorithm for route partitioning is implemented by selecting from two different heuristic algorithms, which are used to solve maximum-cut problems. Chapter 3 also presents the performance of the route partitioning scheme, which is extensively evaluated. Partitioning results from the implementation algorithms are compared and several aspects of the model performance are investigated through different parameter settings.

Chapter 4 presents the path exchanging scheme for 1+1 protected EONs. The static path exchanging optimization problem is defined and formulated into an ILP. Its relation to the two-dimensional bin packing problem is discussed.

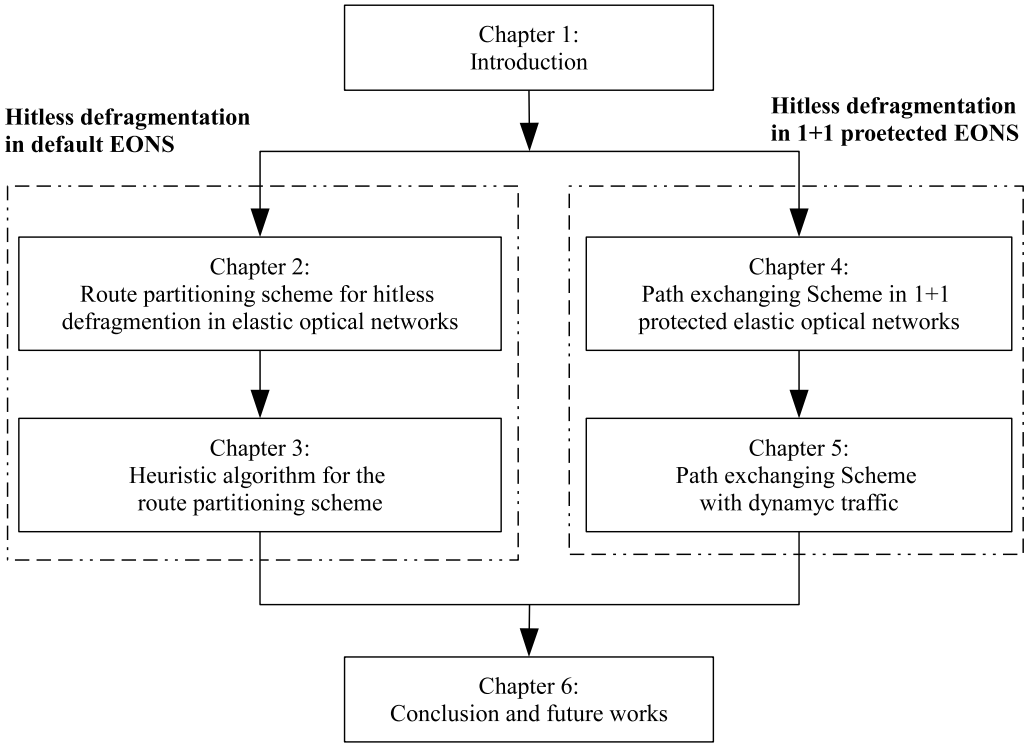


**Figure 1.7:** Organization of the thesis

The static path exchanging problem is formulated into an ILP and proven to be NP-complete.

The path exchanging is considered for dynamic traffic situations in Chapter 3. An approach to implement the path exchanging scheme for a dynamic spectrum defragmention is discussed and a heuristic algorithm is proposed. and a heuristic algorithm presented. The traffic load performance, which is presented in term of bandwidth blocking probability, and the number of switching and reallocation operation are evaluated through different settings.

Chapter 6 concludes the thesis by summarizing the findings and showing the direction for future work.

# Chapter 2

# Route partitioning scheme for hitless defragmention in elastic optical networks

## 2.1 Introduction

This section presents a route partitioning scheme for a proactive push-pull hitless defragmentation in order to increase the amount of allowable traffic in EONs. The presented scheme uses the first-last fit allocation with the route partitioning to further the possibilities of lightpath retuning by avoiding end of line situations caused by retuning interference among connections. End of line occurs when a lightpath could not be moved to its intended index without jumping part of the spectrum. This is due to lightpath enabled to be gradually moved only as far as to the next spectrum index being used on one of its links.

To be able to gradually retune a lightpath whenever it is possible without recurring to spectrum jump, the route partitioning with first-last fit allocation is considered. It offers more options than the first fit allocation. In particular, the route partitioning used as a side selection policy reduces the retuning time and avoids end of lines by limiting the lightpath interferences. Whereas the conventional scheme is limited with all lightpaths stacked one over the other; it is likely to have a lightpath blocked by the interference of another one.

We define the route partitioning problem as an optimization problem. We formulate it with an integer linear programming (ILP) problem. We prove that the route partitioning problem is NP-hard. A heuristic algorithm is introduced for large networks, where the ILP to represent the route partitioning is not tractable. We evaluate the proposed scheme through different networks and varied retuning speed. The results indicate that it reduces the bandwidth blocking probability in EONs and allows for additional traffic load compared to the first fit.

## 2.2 Route partitioning scheme

### 2.2.1 Overview

With the objective to increase the admissible traffic in the network, we aim to minimize the BBP in dynamic EONs. The proposed route partitioning scheme considers hitless defragmentation with the first-last-fit allocation. Hitless defragmentation allows us to tackle spectrum fragmentation without any effect on the ongoing traffic, and the route partitioning helps to reduce end-of-line situations, and furthers the defragmentation possibilities.

Using hitless defragmentation, the wavelength allocated to an active lightpath is retuned to a new spectrum index, where it can fill in the gap within the spectrum. This leads to increased slot blocks availability. However, this spectrum reconfiguration procedure is performed between request arrivals and the time needed to perform the retuning affects its result. The speed at which the retuning is executed impacts on the performance of hitless defragmentation [46]. The time needed to retune a lightpath from an initial wavelength to a new wavelength is considered as a combination of two limitation factors: (i) physical as the speed limit at which the equipments can perform the retuning ($\alpha$ time per retuning step), and (ii) operational ($\beta$) for operations, such as synchronization. We formulate the retuning time for a lightpath as

$$t_{ret} = \alpha \times s + \beta, \tag{2.1}$$

where $s$ is the distance between the spectrum index of initial wavelength and the spectrum index of new wavelength.

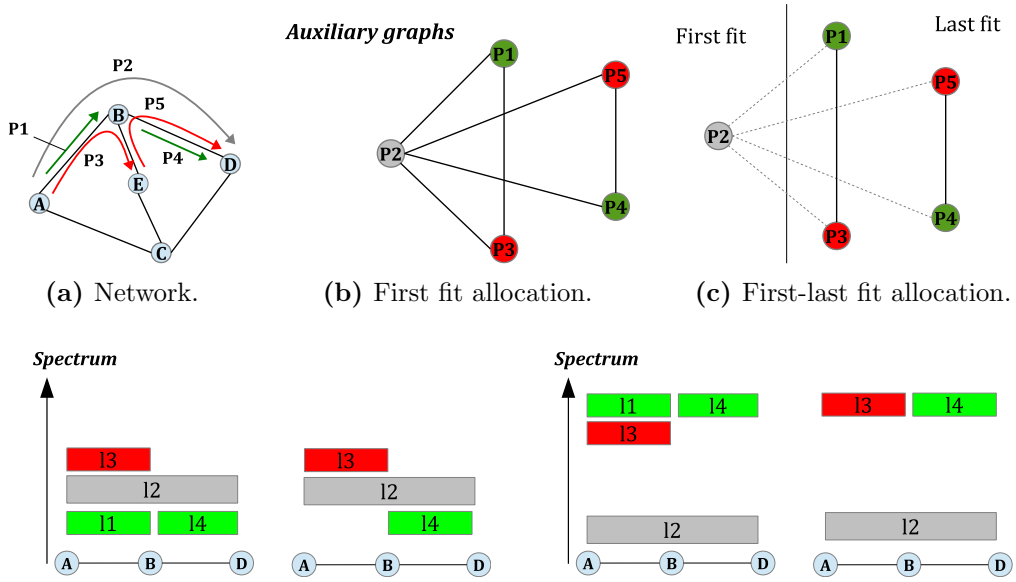


(a) Network. (b) First fit allocation. (c) First-last fit allocation.

(d) First fit (Before and after l1 expires). (e) First-last fit (Before and after l1 expires).

**Figure 2.1:** Route partitioning as selection policy.

The first-last fit allocation policy reduces the retuning distances due to the reduced number of lightpaths that need to be retuned in one direction or the other. Our approach takes advantage of this. Furthermore, we adapt the route partition as side selection policy, where the routing paths and the partitions are selected to avoid lightpath interferences, thus managing end-of-line situations. With the multitude of offered routing possibilities in mesh networks, we define an optimization problem to find the combination of routing paths and route partitioning, which minimize the probability of lightpath interferences.

The concepts of our introduced route partitioning approach are presented as follows.

### 2.2.2 Route partitioning (RP)

In the proposed scheme, we aim to define a bipartition that minimizes the interferences among lightpaths while using the first-last fit allocation. The partitioning is determined along side the routing paths selected for the route requests. The

spectrum bandwidth allocated to each lightpath request depends on which partition its routing path belongs to. The allocation can be either first fit or last fit.

The approach is to use an auxiliary graph where the routing paths are considered as nodes and the routes that share a link are connected by an edge. The partitions are set by seeking for a cut to take advantage of the separation offered by the first-last fit allocation. The cut is defined by the set of edges that have their two edge endpoints in different sets. Given the first-last fit allocation, we use a bipartition where lightpaths with routing path in one partition set are allocated using first-fit and the other lightpaths using last fit allocation. This way, lightpaths with routing paths in different partitions cannot interfere with each other. Therefore, the more there are edges in the cut the more potential lightpath interference we avoid with the partitioning.

With the effect of the cut in mind, we seek to minimize the interferences among routes within the same side of the cut; the edges that are not in the cut represent the remaining interferences between lightpaths allocated on the same side. For that, we seek the routing and partitioning that minimize the total interferences from edges that does not belong to the cut. In other words, we want to determine the routing that, when translated into an auxiliary graph, has the lowest interferences among routes after the cut is defined.

We define the edge cost of the auxiliary graph as the interference penalty to favour the grouping of some routes over others. Two different parameters are considered, namely the ratio of uncommon links between routes and the traffic load for different source-destination pair. When using the ratio of uncommon links as edge cost between two routes, we aim to group the lightpaths that have parallel routings. It is given by the ratio of the number of links not shared by the routes over the number of links used by the two routes. On the other hand, with the traffic load, the grouping is set with regard to the probability of having simultaneous active traffic. With the traffic consideration, each source/destination pair $p = (s, d)$ is assigned a traffic load $\rho_p = \lambda_p \times H_p$, which is measured in Erlang, where $\lambda_p$ is the average arrival rate of the connection requests and $H_p$ is the average holding time of connections. The network's overall traffic load is given

**Table 2.1:** List of notations for RP formulation

| | |
|---|---|
| $G(V, E)$: | Directed graph where $V$ is a set of nodes, and $E$ is a set of links. |
| $P$: | Set of routes, $p \in P$. |
| $w_{pq}$: | Edge cost on auxiliary graph. |
| $y_{pq}$: | Binary variable, 1 if routes $p$ and $q$ share at least a link, and 0 otherwise. |
| $d_{pq}$: | Binary variable, 1 if routes $p$ and $q$ are in different side of the cut, and 0 otherwise. |
| $x_{ij}^{p}$: | Binary variable, 1 if route $p$ use link $(i, j)$, and 0 otherwise. |
| $k_{pq}$: | Binary variable, 1 if routes $p$ and $q$ share a link, and are in same side of the cut, and 0 otherwise. |

by $\rho = \sum \rho_p$. In this setting, the edge cost between source/destination pairs $p$ and $q$ is defined by $\frac{\rho_p * \rho_q}{\rho^2}$.

Figure 2.1 illustrates the principle of the route partitioning. It shows how the two-side selection using the first-last fit with the route partitioning affects the spectrum compared to the first fit allocation. In this example, the routing paths $P_i$ are presented in Fig. 2.1(a). Figures 2.1(b) and (c) represent the derived auxiliary graphs, respectively for the first-fit and the first-last fit. By assigning $p2$ in one partition and $p1$, $p3$ to $p5$ in the other partition (see Fig. 2.1(c)), we allocate lightpaths $l2$ (routed through $p2$) using first fit and lightpaths $l1$, $l3$, and $l4$ (respectively routed through $p1$, $p3$ and $p4$) using last fit. As a result, the end-of-line situation that arises in the first fit allocation (see Fig. 2.1(d)) is avoided with the first-last fit allocation (see Fig. 2.1(e)).

Note that, this paper considers all lightpaths that are from the same source to the same destination to follow the same route. If multiple end-to-end routing paths are considered in order to distribute the traffic load, the proposed scheme can still be applied. That is, given the number of possible alternate routes is set as a parameter, each alternate route is a new routing candidate for the route partitioning. This paper focuses on single end-to-end routing path to present and evaluate the proposed scheme.

### 2.2.3 ILP formulation

We formulate the RP optimization problem as an ILP in order to minimize the total interferences after the cut. The inputs are the source/destination pairs $p = (s, d)$ requesting routing paths and the interference cost between them. Our formulation consists of three parts, (i) determining the routing, (ii) constructing an auxiliary graph where the routes are the nodes and those sharing a link are connected with an edge, and (iii) defining the cut from the resulting auxiliary graph.

We summarize the used notations in Table 2.1. The network is represented as a directed graph $G(V, E)$, where $V$ is a set of nodes, and $E$ is a set of links. Let $P$ denotes the collection of all route requests $p = (s, d)$. The interference cost between routes $p$ and $q$ is given by $w_{pq}$. The outputs are the routing path $x_{ij}^p$ and the partitions are given by $d_{pq}$ for all routes $p = (s, d)$. $d_{pq}$ is set to 1 if route $p$ and $q$ are in different partitions.

$d_{pq}$, $y_{pq}$, $x_{ij}^p$, $k_{pq}$ are used as binary decision variables. $d_{pq}$ is equal to 1 if routes $p$ and $q$ are in different sides of the cut, and 0 otherwise. $y_{pq}$ is equal to 1 if routes $p$ and $q$ share a same link, and 0 otherwise. If link $(i, j)$ is used for route $p$, then $x_{ij}^p$ is equal to 1, and 0 otherwise; $k_{pq}$ is equal to 1 if routes $p$ and $q$ share a link and are in the same side of the cut.

The objective of the optimization problem is to minimize the total interferences among nodes sharing partitions after the cut. Its function is represented by Eq. (2.2).

$$\min \sum_{p,q} (1 - d_{pq}) y_{pq} w_{pq} \tag{2.2}$$

Since Eq. (2.2) is not a linear form, the equivalent Eq. (2.2a) is used for the ILP formulation. Variable $k_{pq}$ is introduced with constraints (2.2g)-(2.2i) to pass from quadratic to linear formulation.

$$\min \sum_{1 \le p < q \le |P|} w_{pq} \times k_{pq} \tag{2.2a}$$

Subject to

$$\sum_{j \in V:(i,j) \in E} x_{ij}^p - \sum_{j \in V:(j,i) \in E} x_{ji}^p = 1$$
$$\forall\, p = (s,d) \in P, i \in V, i = s \tag{2.2b}$$
$$\sum_{j \in V:(i,j) \in E} x_{ij}^p - \sum_{j \in V:(j,i) \in E} x_{ji}^p = 0$$
$$\forall\, p = (s,d) \in P, i \in V, i \neq s, d \tag{2.2c}$$
$$d_{pq} + d_{pk} + d_{qk} \le 2 \;\; \forall\, 1 \le p < q < k \le |P| \tag{2.2d}$$
$$d_{pq} - d_{pk} - d_{qk} \le 0 \;\forall\, 1 \le p < q \le |P|, \;\; k \neq p, q \tag{2.2e}$$
$$x_{ij}^p + x_{ij}^q - 1 \le y_{pq} \;\; \forall\, (i,j) \in E, \; p, q \in P \tag{2.2f}$$
$$k_{pq} \le y_{pq} \;\; \forall\, p, q \in P \tag{2.2g}$$
$$k_{pq} \le 1 - d_{pq} \;\; \forall\, p, q \in P \tag{2.2h}$$
$$k_{pq} \ge y_{pq} - d_{pq} \;\; \forall\, p, q \in P \tag{2.2i}$$
$$x_{ij}^p = \{0,1\} \;\; \forall\, (i,j) \in E, p \in P \tag{2.2j}$$
$$y_{pq}, d_{pq}, k_{pq} = \{0,1\} \;\; \forall\, p, q \in P \tag{2.2k}$$

Eqs. (2.2b) and (2.2c) represent the traffic flow constraint. They ensure that all traffic leaving a source node are routed to destination without any traffic lost. The constraint on the destination node is not added as it has been proved to be redundant when the constraints at the source in Eq. (2.2b) and the intermediate nodes in Eq. (2.2c) are stated [66]. Eq. (2.2f) defines the auxiliary graph from the routing paths. It sets $y_{pq}$ to 1 if routes $p$ and $q$ share at least a link $(i,j)$, otherwise it is forced to 0 ($x_{ij}^p = 0$ or $x_{ij}^q = 0$ on all $(i,j)$ links). Eqs. (2.2d) and (2.2e), called triangle inequalities, introduce the cut [67]. The triangle inequalities induce facets of the cut, where every three nodes define a facet, which either does or does not intersect with the cut plane. When a facet intersects with the cut plane, two of its nodes are in one side of the cut and the last one is in the opposite side. Therefore, for the two nodes in the same side, $d_{pq}$ is equal to zero; in Eq. (2.2d) the sum of $d_{pq}$ is less or equal to 2. Eq. (2.2e) guaranties that $d_{pq}$ is equal to 1 for nodes in opposite sides. When a facet does not intersect with the

cut plane, $d_{pq}$ is equal to zero for all pairs, which does not contradict Eqs. (2.2d) and (2.2e). When possible, facets are forced to intersect with the cut to minimize path interference. Eq. (2.2f) puts $y_{pq}$ to 1 if paths $p$ and $q$ share the same link. Eqs. (2.2g)-(2.2i) define the remaining edges after the cut. They set $k_{pq}$ to zero if routes $p$ and $q$ are not connected ($y_{pq} = 0$) or are allocated to different sides of the cut ($d_{pq} = 1$).

### 2.2.4 NP-hardness of RP

This subsection proves that the RP problem is NP-hard. Since RP is an optimization problem, its NP-hardness is proved by proving that the RP decision problem defined below is NP-complete.

**Definition 1** *The RP decision problem (RPD). Given a network $G(V, E)$, a set of route requests $P$, and a real number $h$, is it possible to define all routes in $P$ through $G(V, E)$ and partition them with at most $h$ total interference?*

**Theorem 1** *RPD is NP-complete.*

**Proof 1** *The following proves Theorem 1.*

RPD is in NP, as we can verify in polynomial time that a given routing and partitioning instance of the RPD has at most $h$ total interference. The time complexity to verify it is $O(|P|^2)$.

We show that the maximum cut decision problem (max-cut), a well known NP-complete problem [68], is polynomial time reducible to RPD. Max-cut is defined as: is there a bipartition of the nodes in a given graph $G_c(V_c, E_c)$ such that the total capacity of edges with two endpoints in different sets is at least $k$, which is a given number?

First, we construct an instance of RPD from any instance of max-cut in polynomial time. An instance of max-cut is expressed by $G_c(V_c, E_c)$, $k$, $w_{pq}$, $y_{pq}$ and $d_{pq}$, where $(p, q) \in E_c$. $w_{pq}$ is the link capacity. $y_{pq}$ is equal to 1 if nodes $p$ and $q$

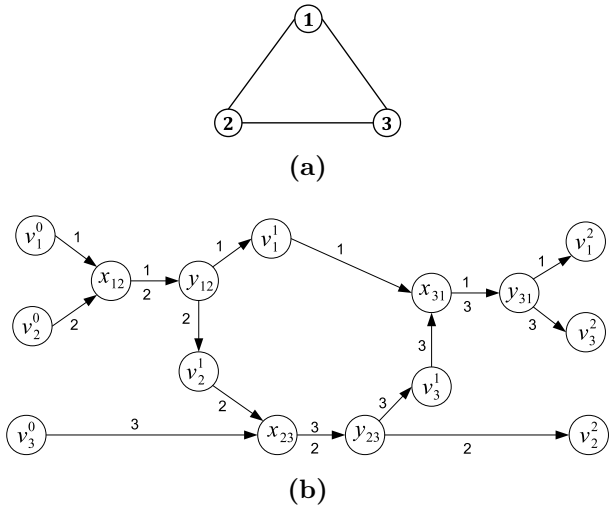


**Figure 2.2:** Polynomial reduction (a) Max-cut graph. (b) Translated to RP network.

adjacent, and 0 otherwise. $d_{pq}$ is set to 1 if nodes $p$ and $q$ are on different sides of the cut, and 0 otherwise.

We apply the idea of the transformation in [69], which translates any instance of the graph coloring problem to an instance of the static lightpath establishment problem. In our case, we seek the cut capacity, which is the total capacity of edges with two endpoints in different sets, instead of the number of colors. Using the same polynomial time algorithm as in [69], we translate any graph $G_c(V_c, E_c)$, for which we seek the cut capacity, into a network $G'(V', E')$ in which we apply RPD as follows (See an example in Fig. 2.2):

1. Create node $v_i^0$ for every node $i \in V_c$.

2. For every edge $e = (i, j) \in E_c$: create four new nodes $x_{ij}$, $y_{ij}$, $v_i^r$, $v_j^l$ and directed edges $v_i^{r-1} \to x_{ij}$, $v_j^{l-1} \to x_{ij}$, $x_{ij} \to y_{ij}$, $y_{ij} \to v_i^r$, $y_{ij} \to v_j^l$. $r$ and $l$, which are initialized to 0 in 1), are incremented for $v_i^r$ and $v_j^l$, respectively, when edge $e = (i, j)$ is considered.

The complexity of this algorithm is $O(|E_c|)$.

Every node on $G_c(V_c, E_c)$ is translated, for RPD, into a route $p = (v_i^0, v_i^n)$, where $n$ is the number of nodes adjacent to node $p$ on $G_c(V_c, E_c)$. If two nodes

$p$ and $q$ on $G_c(V_c, E_c)$ are adjacent, the corresponding routes share a link in the translated network $G'(V', E')$. If the nodes are separated on different sides of the cut on $G_c(V_c, E_c)$, the corresponding routes $p$ and $q$ are allocated on different partitions in $G'(V', E')$. Therefore, $y_{pq} = 1$ if routes $p$ and $q$ share a link, and $d_{pq} = 1$ if routes $p$ and $q$ are allocated on different partitions. The interference between routes $p$ and $q$ is set to $w_{pq}$ if routes $p$ and $q$ share a link, and 0 otherwise. To complete the instance of RPD, we define $h'$ as

$$h' = \sum_{(p,q)\in E_C} w_{pq} \quad - \quad k. \tag{2.3}$$

In the following we show that with this transformation algorithm, if a max-cut instance is feasible, then the corresponding RPD instance is feasible.

Suppose a max-cut instance is a feasible instance. It means

$$\sum_{(p,q)\in E_c} d_{pq} w_{pq} \quad \geq \quad k. \tag{2.4}$$

If we subtract the terms of this equation from $\sum_{(p,q)\in E_c} w_{pq}$, then we have

$$\begin{aligned} \sum_{(p,q)\in E_c} (1 - d_{pq}) w_{pq} \quad &\leq \quad \sum_{(p,q)\in E_c} w_{pq} - k \\ &= \quad h'. \end{aligned} \tag{2.5}$$

Since $y_{pq}$ is equal to 1 if $(p, q) \in E_c$ and 0 otherwise, $y_{pq} w_{pq}$ is equal to $w_{pq}$ if $(p, q) \in E_c$ and 0 otherwise. Therefore, we can replace $w_{pq}$, where $(p, q) \in E_c$, by $y_{pq} w_{pq}$, where $p, q \in P$. This gives us

$$\sum_{p,q\in P} (1 - d_{pq}) y_{pq} w_{pq} \quad \leq \quad h'. \tag{2.6}$$

The left hand side of Eq. (2.6) is, as expressed in Eq. (2.2), the total interference after partitioning in $G'(V', E')$, translated from $G_c(V_c, E_c)$. Therefore, Eq. (2.6) establishes that if the max-cut instance is a feasible instance, then the total interference of the RPD instance is at most $h'$. To conclude that the RPD instance is a feasible instance, we verify that the routing of all routes in $P$ exist in the network $G'(V', E')$. This is true, since the transformation algorithm defines a

unique routing for each route request. Thus, if the max-cut instance is feasible, then the RPD instance is feasible.

Finally, to complete this proof, we show that if a RPD instance in $G'(V', E')$ is feasible, then the corresponding max-cut instance in $G_c(V_c, E_c)$ is feasible. Suppose that an instance of RPD is feasible in $G'(V', E')$, then Eq. (2.6) is verified. By taking the opposite direction of the previous approach to verify that Eq. (2.4) leads to Eq. (2.6), we show that Eq. (2.6) leads to Eq. (2.4). With Eq. (2.6) verified, the max-cut instance is feasible in $G_c(V_c, E_c)$. Thus, if the RPD instance in $G'(V', E')$ is feasible, then the max-cut instance in $G_c(V_c, E_c)$ is feasible. ■

# 2. ROUTE PARTITIONING SCHEME FOR HITLESS DEFRAGMENTION IN ELASTIC OPTICAL NETWORKS

# Chapter 3

# Heuristic algorithm for the route partitioning scheme

## 3.1 Heuristic algorithm

### 3.1.1 Load balanced routing with minimum cut algorithm

We introduce a heuristic algorithm for large network where the ILP for the RP problem is not tractable. The presented heuristic algorithm is a relaxation of the RP problem by decomposing it into two separate problems solved sequentially, namely (i) the load balancing problem and (ii) the maximum cut problem. The load balancing problem is solved using an ILP tractable for considered networks. The maximum cut problem is solved using a heuristic algorithm. We translate the routing paths yielded by the load balancing problem to an auxiliary graph that is used as input for the maximum cut problem. The heuristic algorithm (algorithm 1), which is referred to as load balanced routing with minimum cut (LBR-MC), is described below.

In step 1, we determine all the routing paths by using load balanced routing in order to minimize the number of routes sharing the same link (minimum used indexes). We formulate the load balanced routing as the following ILP. The objective to minimize in Eqs. (3.0a) and (3.0b) is the number of used indexes. It is subject to the traffic continuity constraint in Eqs. (3.0c) and (3.0d).

**Algorithm 1:** LBR-MC heuristic Algorithm.

**Input**: Network, set of routes

**Output**: Routing and partitions

1. **Step 1:** Determine routing paths with LBR
2. **Step 2:** Draw auxiliary graph from routes
3. **Step 3:** Define partitions
4. **3.1:** Find maximum cut
5. **3.2:** Set partition for maximum cut

$$\min \quad M \tag{3.0a}$$

Subject to

$$\sum_{p \in P} x_{ij}^p \leq M \qquad \forall\ (i,j) \in E \tag{3.0b}$$

$$\sum_{j \in V:(i,j) \in E} x_{ij}^p - \sum_{j \in V:(j,i) \in E} x_{ji}^p = 1 \qquad \forall\ p = (s,d) \in P, i \in V, i = s \tag{3.0c}$$

$$\sum_{j \in V:(i,j) \in E} x_{ij}^p - \sum_{j \in V:(j,i) \in E} x_{ji}^p = 0 \qquad \forall\ p = (s,d) \in P, i \in V, i \neq s, d \tag{3.0d}$$

$$x_{ij}^p = \{0,1\} \quad \forall\ (i,j) \in E, p \in P \tag{3.0e}$$

In case the ILP for load balancing is not tractable for considered networks, the algorithm for physical paths allocation presented in [70] can be used. The steps of the algorithm in [70] are described in the following. i) All the source-destination pairs are randomly sorted and routed through the first found minimum-hop path. ii) For each pair considered, an alternative minimum-hop path substitutes the one previously assigned if and only if the number of channels (congestion) of the most loaded link in the alternative path is lower than the congestion of the most loaded link in the previously assigned path. This process is repeated for all node-pairs. iii) Repeat step ii) until no more substitution is possible.

In step 2, we draw an auxiliary graph from the defined routing paths. A node of the auxiliary graph expresses a route, and an edge of the auxiliary graph expresses that the two nodes connected by it share a physical link.

In step 3, we determine the route partitioning using the auxiliary graph as input. We seek the maximum cut, and then separate the routes that are allocated using first fit from the routes that are allocated using last fit. Since the maximum cut problem is NP-complete [68], we use approximation algorithms to determine the cut. In order to obtain a cut close to the optimal one, we repeat the used approximation algorithm several times with varied initial settings. The setting that yield the best cut is then used to determine the route partitioning. The two approximation algorithms considered to determine the maximum cut are described in the following.

#### 3.1.1.1 Local search algorithm

The first algorithm we consider to find a suitable cut is a local search algorithm [71]. The local search algorithm can be resumed as follows:

i. Start with an arbitrary partition (for example, $\varphi$).

ii. Pick a node $v$ such that moving it across the partition would yield a greater cut value.

iii. Repeat step *ii* until no such $v$ exists.

Since the cut result of the local search depends on the initial settings (partition $\varphi$), we run the algorithm with varied initial settings and choose the ones that yield the best cut. Then, we define the partitioning using those settings.

#### 3.1.1.2 Goemans/Williamson randomized approximation algorithm

The second considered algorithm is the Goemans/Williamson randomized approximation (GWRA) algorithm for max-cut. The GWRA is a semi definite programming (SDP) approximations algorithm that runs in polynomial time. The SDP formulation is a relaxation of the max-cut MILP formulation, which

cannot be solved in polynomial time. With the SDP, the decision variables are unit vectors $x_u \in \Re^n$ instead of integers $x_u \in \{-1, 1\}$.

$$\max \sum_{(u,v)\in E} w_{uv}(1 - x_u \cdot x_v) \tag{3.1}$$

Subject to

$$\begin{aligned} x_u \cdot x_u &= 1 \qquad \forall\, u \in V \\ x_u &\in \Re^n \qquad \forall\, u \in V \end{aligned}$$

The GWRA algorithm can be summarized as follows:

1. Solve the SDP given by Eq. 3.1 to obtain vectors $x_u$
2. Pick a random unit vector $\alpha \in \Re^n$
3. Output $\{v \mid x_v \cdot \alpha > 0\}$

Solving the SDP relaxation problem returns the vectors $x_u \in \Re^n$. Any unit vector $\alpha \in \Re^n$ is in a plan that partitions the set of vectors $x_u$ in two sets. Therefore, it is necessary to consider several $\alpha$, in order to return the best cut, even though any $\alpha$ would yield a cut at least 87.8% of the optimal cut [72]. The vectors $x_u$ in one side of the cut are determined by computing $x_v \cdot \alpha$. The output nodes $v$ represent the routing paths that are allocated using the first fit allocation. The remaining paths are allocated using the last fit allocation.

### 3.1.2 Computational time of max-cut approximation algorithms

The Goemans-Williamson algorithm has a computational running time of $O(|V|^{3.5} \log \frac{1}{\epsilon})$ when the interior point methods is used to solve the SDP relaxation. $\epsilon$ is the desired accuracy. In comparison, the local search algorithm has a computational running time of $O(|V||E|)$ for unweighed graph. In the case of weighted graph, it can be exponential to $|V|$. However it can be modified to run in $O(\frac{1}{\epsilon}|V| \log |V|)$ iterations of the improvement step.

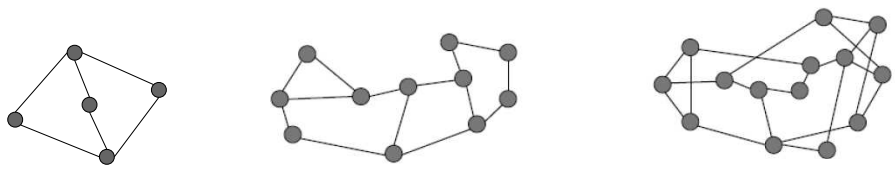

(a) Five-node (b) Abilene (c) NSFNet

**Figure 3.1:** Simulation networks.

## 3.2 Results and discussions

### 3.2.1 Simulation settings

We evaluate the bandwidth blocking probabilities of the proposed route partitioning scheme through simulation to assess the allowable traffic load. We compare the proposed scheme to the conventional push pull retuning with first-fit [51] and a random first-last fit allocation policies. We investigate the effect of the retuning speed on the proposed scheme with varied values of $\alpha$ (See Eq. (2.1), $\alpha$ in ms and $\beta$ supposed to be fixed and negligible). The effect of end-of-line and its correlation with the number of performed retuning operations are also investigated.

The following assumptions are considered for purpose of simulation. The channel spacing and the total number of spectrum subcarrier slots per channel are considered as 12.5 GHz and 400, respectively. The connection requests are generated randomly based on a Poisson distribution process ($\lambda$) and the holding time of connection requests follows an exponential distribution ($H = 1/\mu$). The traffic load is given in Erlang by $\rho = \lambda * H$. The source and destination of each request are supposed to be independent from the previous ones and the number of requested lightpaths is uniformly distributed from 1 to 16. We run the simulation for 200 different seeds, with each of which 10000 lightpath connection requests are generated. The interval of confidence of reported results is 95%. The three networks presented in Fig. 3.1 are used as simulation supports. The Abilene and the NSFNet networks, are commonly used for backbone simulations [73]. In addition, for comparison purpose, we generated random networks refereed to as rand-net i-j, where $i \in \{8, 9, 10\}$ is the number of nodes, and $j \in \{3, 4, 5\}$ is the average node degree.

**Table 3.1:** Cuts of auxiliary graph obtained by algorithms for different networks

| Networks | Local-search | GWRA | Optimal by MILP | |
|---|---|---|---|---|
| | Cut (Links) | Cut (Links) | Cut | Bound (Gap) |
| Five-node | 20(8) | 20(8) | 20 | 20 |
| Abilene | 232(72) | 232(72) | – | – |
| NSFNet | 2291(436) | 2293(436) | – | – |
| Rand-net 8-3 | 208(50) | 208(52) | 208 | 208 |
| Rand-net 8-4 | 126.5(34) | 126.5(35) | 126.5 | 126.5 |
| Rand-net 8-5 | 32(16) | 32(16) | 32 | 32 |
| Rand-net 10-3 | 349(92) | 347(92) | – | – |
| Rand-net 10-4 | 204(65) | 204(65) | 204 | 204 |
| Rand-net 10-5 | 314.5(74) | 314.5(74) | 314.5 | 316(0.51%) |
| Rand-net 12-3 | 1255(246) | 1553(245) | – | – |
| Rand-net 12-4 | 438(121) | 437(121) | – | – |
| Rand-net 12-5 | 271(83) | 271(84) | – | 272.33(–) |

### 3.2.2 Cut comparison between approximation algorithms and ILP

We compare, for the different networks, the value of the cut obtained form the different approximation algorithms. The results are presented in table 3.1. We provide also the value of the cut or an upper bound computed using a max-cut MILP when tractable. Note that we have solved the MILP with the CPLEX solver [74], and the SDP relaxation problem using the SCDP library for semidefinite programming [75], and that the formulation of the MILP for max-cut is not included in this paper.

Table 3.1 shows that, despite the difference of approximation factors, the cuts obtained by the two approximation algorithms are similar and are almost the same as the one returned by the MILP when tractable. Furthermore, the local search algorithm yield better cuts than the GWRA in some cases. This can be explained by the fact that the approximation factors are just an indication of how close to the optimal value the returned approximations are guaranteed to be for the worst case. In reality, the algorithms return approximation values closer to

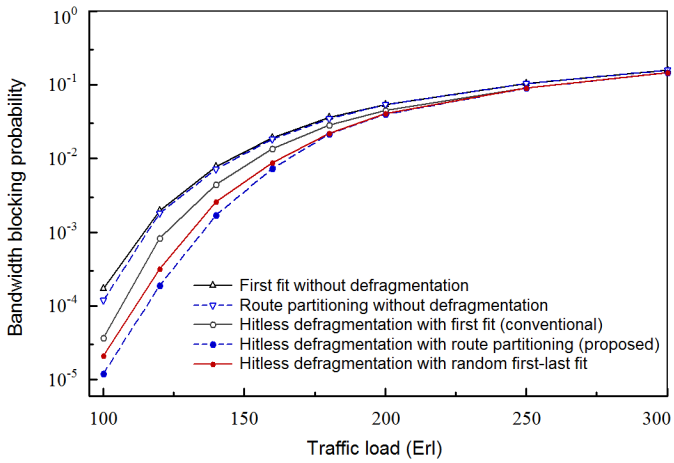


**Figure 3.2:** Bandwidth blocking probability of proposed scheme compared with the conventional first fit and a random first-last fit ($\alpha = 0.05$ms).

**Table 3.2:** Number of variables solving the ILP for RP with CPLEX solver

| Networks | Binaries | Rows | Column | Nonzeros |
|---|---|---|---|---|
| Five-node | 1845 | 17405 | 1845 | 51795 |
| Abilene | 21065 | 618585 | 21065 | 1846065 |
| NSFNet | 57421 | 2753023 | 57421 | 8233901 |

the optimal value than the approximation factor indicates. In particular, both heuristic algorithms prove to be quit efficient for the auxiliary graphs relative to the networks we have considered.

Note that, for the remainder, the cut and route partitioning used for the five-node network are computed by the ILP formulation that solve the RP problem. For the remaining networks, we use the LBR-MC heuristic algorithm due to the NP-hardness of RP problem (See Table 3.2). Therefore, all results presented for the proposed scheme in the five-node network are obtained by mean of the ILP and the results for networks 2 and 3 are obtained by the heuristic. In our evaluation of the five-node network, the heuristic algorithm yields the same route partitioning as the ILP.

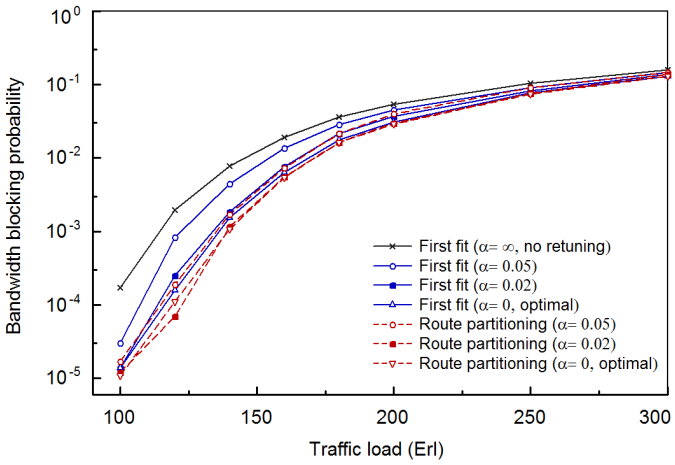


**(a)** Five-node

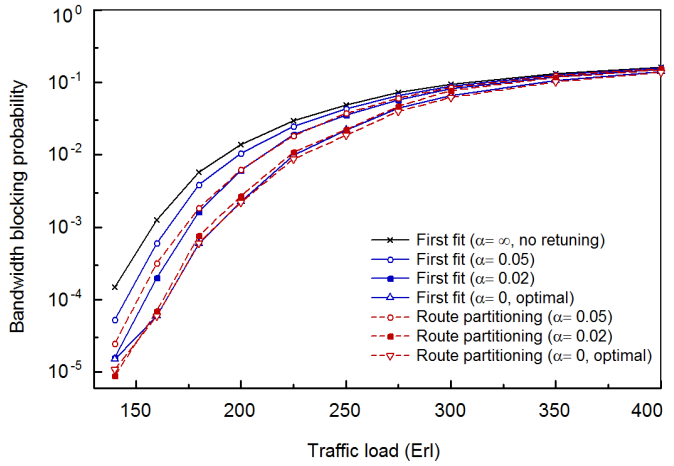


**(b)** Abilene

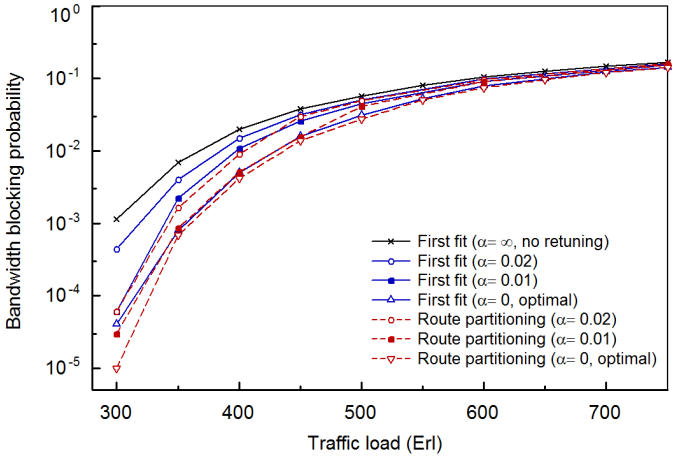


**(c)** NSFNet

**Figure 3.3:** Bandwidth blocking probability for hitless defragmentation using the route partitioning compared to the first fit for different returning speeds.

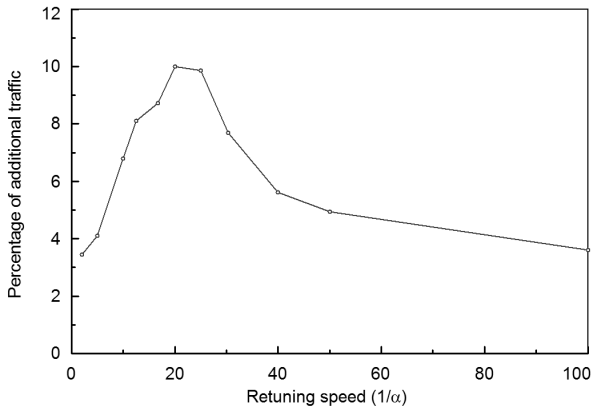


**Figure 3.4:** Dependency of additional traffic (%) of the proposed scheme on the conventional first fit in five-node network.

### 3.2.3 Performance comparison with conventional scheme

#### 3.2.3.1 Bandwidth blocking probability

Figure 3.2 presents the bandwidth blocking probabilities of the proposed route partitioning scheme compared to the conventional push-pull with first fit and a random first-last fit allocation. It shows that the proposed scheme reduces considerably the bandwidth blocking probability and that it outperforms the conventional push pull retuning. The result presented in Fig. 3.2 are from the five-node network and for an $\alpha$ set to 0.05ms.

#### 3.2.3.2 Effect of retuning speed

In Fig. 3.3, we compare the bandwidth blocking probabilities of the proposed scheme and the conventional first fit on different networks for variable retuning speeds. We observe that the bandwidth blocking probabilities of both the route partitioning and the first fit are improved by increasing the retuning speed (decreasing $\alpha$). However, the performances of the route partitioning improve at a higher rate than those of the first fit. When the retuning speed is slow ($\alpha \neq 0$) the effect of the proposed route partitioning using first-last fit is highlighted. When the retuning time is negligible (optimal $\alpha \approx 0$) the route partitioning scheme, while offering better performances, presents no significant improvement

compared to the conventional approach. However, when the retuning time is taken into account ($\alpha \neq 0$), the difference is clearly noticeable. For bandwidth blocking probabilities less than 0.01, the route partitioning offers up to 10% additional traffic compared to the conventional first fit.

#### 3.2.3.3 Additional traffic admissibility

In Fig. 3.4, we study how the relative additional traffic load allowed by the proposed scheme, with regard to the traffic load that is allowed by the conventional scheme, changes according to the retuning speed. The relative added traffic load is computed using the following equation:

$$\text{Added traffic } (\%) = \frac{\rho_1 - \rho_2}{\rho_2} \times 100, \tag{3.2}$$

where $\rho_1$ and $\rho_2$ are the traffic load values taken when the blocking probability is 0.01, respectively for the proposed and conventional schemes. We observe that, when the retuning speed is very low (close to no retuning), the performances of the conventional scheme and the proposed scheme are comparable. However, a slight increase of the retuning speed results in a significant improvement of our scheme compared to the conventional one. This trend continues until the additional traffic reaches a peak and then decreases gradually for higher retuning speed. The proposed scheme, still, offers better results when the retuning speed is high enough for the retuning time to be neglected. This shows that the performances of the conventional push-pull with first fit greatly depend on the retuning speed, while the route partitioning with first-last fit allocation is less subject to it. In other words, hitless defragmentation using the route partitioning with first-last fit can still be effective with reduced retuning speed.

### 3.2.4 Effect of the route partitioning scheme

#### 3.2.4.1 Bandwidth blocking performance

In Fig. 3.5, we weigh the effect of the route partitioning as allocation policy by comparing its results with that of a random first-last fit allocation policy that uses alternate side selection as allocation policy. The results of the random first-last fit allocation policy show the raw benefice of using the first-last fit compared

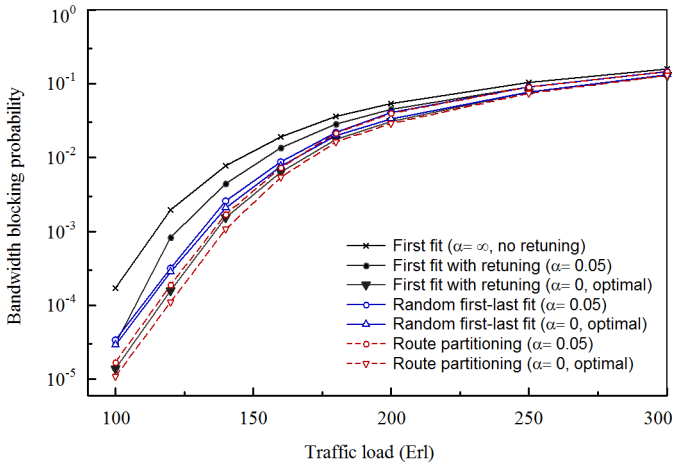


**(a)** Five-node

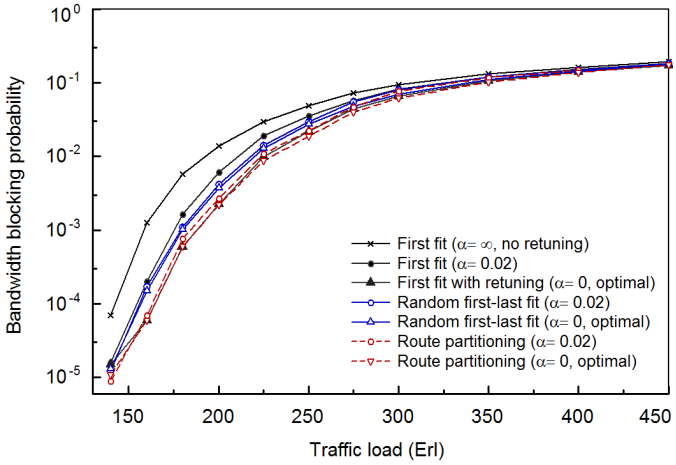


**(b)** Abilene

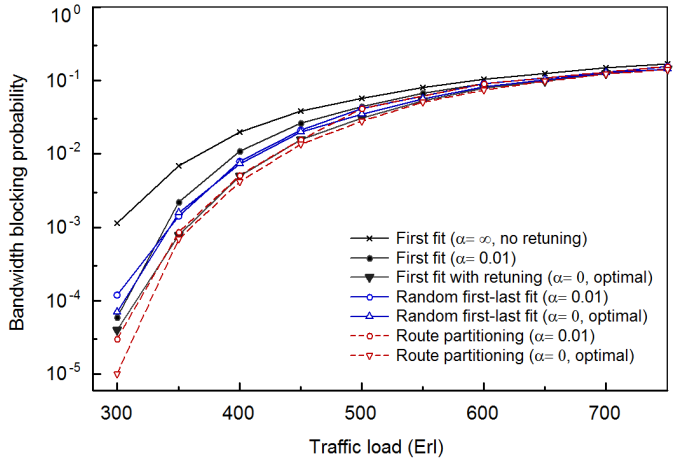


**(c)** NSFNet

**Figure 3.5:** Bandwidth blocking probability of the proposed route partitioning with first-last fit compared to a random first-last fit selection policy.

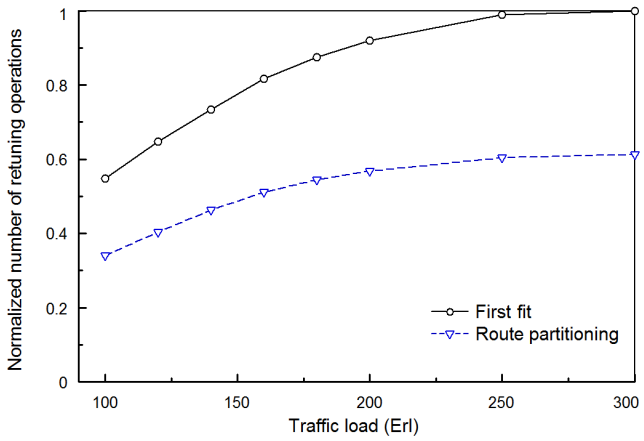


**(a)** Five-node

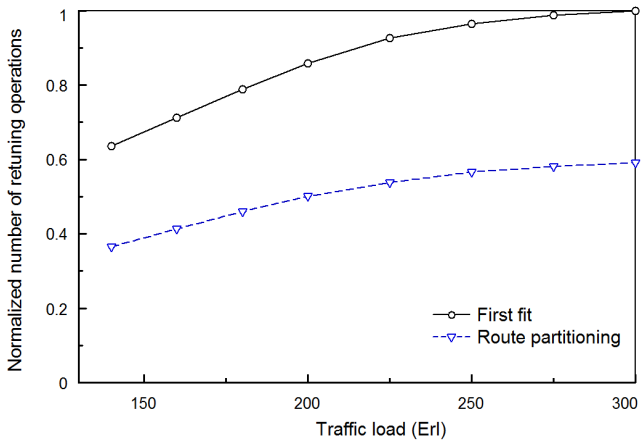


**(b)** Abilene

**Figure 3.6:** Number of required retuning operations normalized to its maximum $(\alpha \approx 0)$ .

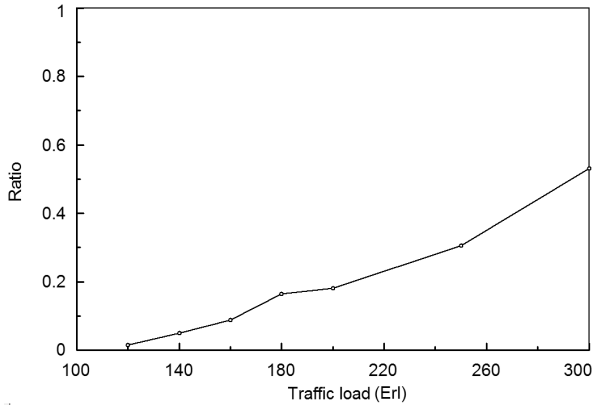


**Figure 3.7:** Ratio of end-of-line occurrences (Five-node).

to the first fit when the retuning speed is not fast enough. Due to the two-side spectrum allocation policy, the number of retuning operations and the retuning distances are reduced (see Fig. 3.6). As a result, the effect of the retuning speed is reduced. However, this also illustrates the fact that without a proper side selection policy, the advantage of the first-last fit is limited. It is shown with the first-fit allocation performing better than the random first-last fit allocation when the retuning speed is fast enough. On the other hand, when we use the route partitioning as side selection policy, the performance of the first last fit policy is always better than that of the first-fit, even if the range of improvement is reduced with higher retuning speed. By avoiding end-of-line situations, the route partitioning guaranties an edge to the first-last fit allocation over the conventional push-pull retuning that uses first fit allocation policy.

#### 3.2.4.2 End-of-line occurrences

We evaluate the number of end-of-line occurrences considering that the retuning speed is fast enough to perform the retuning of a lightpath without delay ($\alpha = 0$). In which case, all retuning operations are performed at once. Therefore, after each retuning, we record an end-of-line occurrence whenever there is a slot block to which a lightpath could be retuned in but is not due to the interference of other lightpath(s). Figure 3.7 presents the ratio of the number of accounted end-of-line situations when the proposed scheme is used to when the first fit is

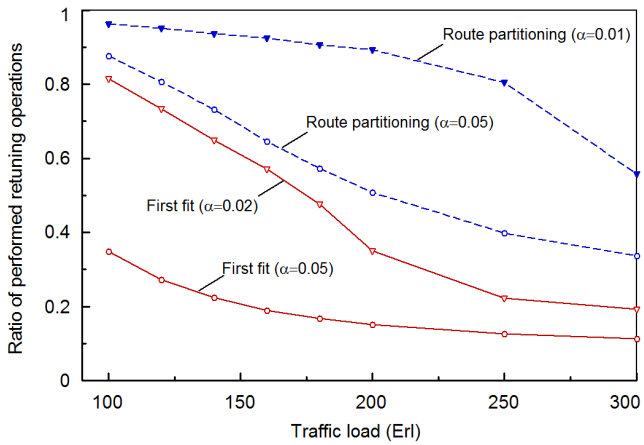


**Figure 3.8:** Ratio of performed retuning operations ($\alpha \neq 0$) to the required retuning operations ($\alpha \approx 0$) in five-node network.

used for a range of traffic loads. It shows that our route partitioning scheme reduces considerably the number of end-of-line situations. Moreover, when put in correlation with Fig. 3.8, it highlights the effect of the end-of-line situations on the retuning capacity when the retuning speed is reduced. With a high number of end-of-line situations, the percentage of performed retuning operations over the necessary number of retuning operations (corresponding to $\alpha \approx 0$) is very low when the retuning speed is low ($\alpha = 0.05$). The low percentage of performed retuning operations also correspond to the cases where the bandwidth blocking probabilities are the farthest from their smallest values (see Fig. 3.3, $\alpha = 0.05$).

### 3.2.5 Effect of parallel retuning

#### 3.2.5.1 Bandwidth blocking performance

We compare the blocking performance of the route partitioning scheme obtained using the GWRA algorithm to the one obtained by the conventional push-pull retuning with first fit when parallel retuning is implemented. In parallel retuning, lightpaths that are link disjoint are allowed to be retuned simultaneously. Figure 3.9 presents the bandwidth blocking probabilities of both schemes with and without parallel retuning. It shows that, when the retuning time ($\alpha$ in time unit) is considered, the route partitioning scheme outperforms the conventional

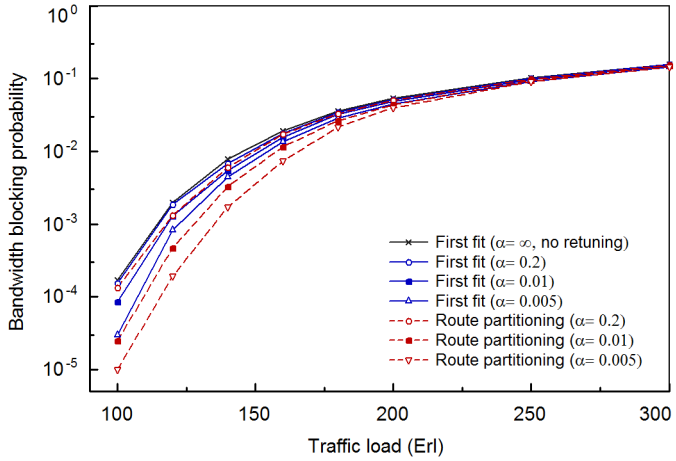


**(a)** Without parallel retuning

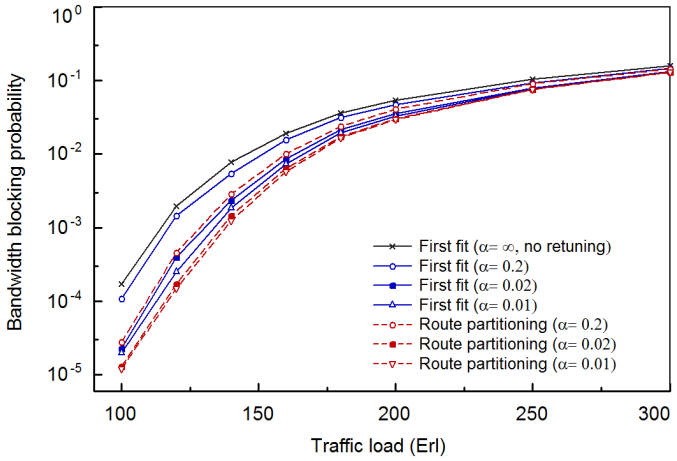


**(b)** With parallel retuning

**Figure 3.9:** Bandwidth blocking probability of route partitioning scheme with or without parallel retuning compared with the conventional first fit in five-node network.

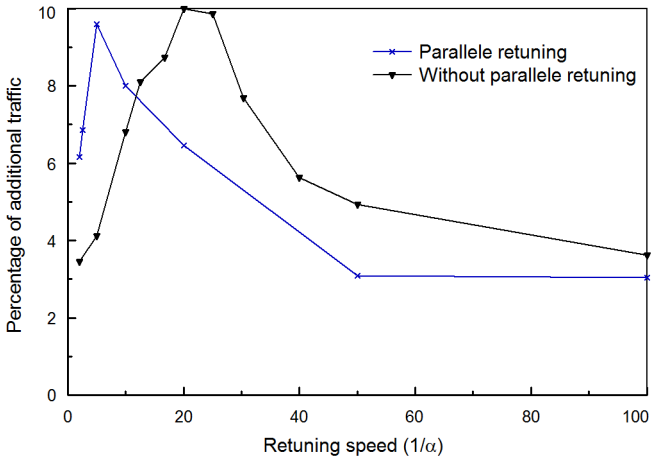


**Figure 3.10:** Dependency of the % of added traffic by the route partitioning over the conventional first fit with regard to the retuning speed (Five-node).

one. The time it takes to retune a lightpath is given by $t_{ret} = \alpha \times s + \beta$, where $s$ is the distance the lightpath is moved and $\beta$ is negligible. Furthermore, it shows that the path partitioning scheme with first-last fit is even less dependent on the retuning speed when parallel retuning is implemented (See route partitioning bbp for $\alpha = 0.2$). The same can be observed in Fig. 3.10.

#### 3.2.5.2 Additional traffic admissibility

In Fig. 3.10, we investigate the maximum relative additional traffic load allowed by the route partitioning compared to the conventional one with regard to the retuning speed. We observe that using parallel retuning further reduces the retuning speed required to achieve high performances with the route partitioning scheme compared to the conventional one. Similar to the case with non-parallel retuning, the gap tends to be reduced as the retuning speed increases. The results of Figs. 3.9 and 3.10 are from the five-node network where the max-cut is optimal for both GWRA and local-search algorithms.

**Table 3.3:** Maximum added traffic in % for different networks

| Networks | % added traffic | Ave. node degree |
|---|---|---|
| Five-node | 9.6 | 2.4 |
| Abilene | 7.92 | 2.55 |
| NSFNet | 7.53 | 3.14 |
| Rand-net 8-3 | 9.28 | 3 |
| Rand-net 8-4 | 4.89 | 4 |
| Rand-net 8-5 | 4.71 | 5 |
| Rand-net 10-3 | 7.22 | 3 |
| Rand-net 10-4 | 3.15 | 4 |
| Rand-net 12-3 | 7.12 | 3 |
| Rand-net 12-4 | 3.08 | 4 |

### 3.2.6 Effect of network characteristics

We investigate the effect of the network characteristics on the benefits of the route partitioning in term of maximum added traffic over the conventional one. The maximum percentage of added traffic obtained through networks with different characteristics are compiled in table 3.3. We observe that, for networks with average node degree below three, the percentage of added traffic is around $7-10\%$. On the other hand, for networks with average node degree of four and above, the added traffic is less than 5%. Furthermore, for networks with the same number of nodes, the maximum added traffic decreases when the average node degree increases. This can be explained by the fact that lightpaths in networks with high average node degree, do not necessarily have to share many links. Therefore, the number of path interferences to be avoided are reduced to begin with. This is illustrated by the number of links that are cut from the auxiliary graph (See Table 3.1). Another factor that influence the effect of the path partitioning scheme is the minimum node degree. The minimum node degree constitute a bottleneck as all paths from/to the node with the minimum degree have to share the same links.

Our results show that end-of-line limits hitless defragmentation by reducing the possibility of retuning. By using the route partitioning it can be reduced,

therefore reducing the bandwidth blocking probability and incidentally increasing the traffic load allowable with a given quality of service threshold.

## 3.3 Summary

Chapters 2 and 3 presented a route partitioning scheme for hitless defragmentation using first-last fit allocation in order to increase the allowable traffic in EONs. The presented scheme increases the possibilities of lightpath retuning by avoiding the retuning interference among lightpaths. The use of first-last fit reduces the number of needed retuning operations and the retuning time, while the route partitioning furthers the possibility of retuning by avoiding end-of-line situations. The route partitioning problem was defined as an optimization problem and an ILP problem was formulated to solve it. The route partitioning problem was proven to be NP-hard, and a heuristic algorithm was presented for large networks, where the ILP to represent the route partitioning is not tractable. The numerical results showed that the proposed scheme offers reduced bandwidth blocking probability with limited retuning speed. Furthermore, the proposed scheme allows up to 10% more traffic compared to the conventional hitless defragmentation.

# Chapter 4

# Path exchanging Scheme in 1+1 protected elastic optical networks

## 4.1 Introduction

This section presents a defragmentation scheme that allows exchanging the primary and backup paths' function in 1+1 path protected EONs. By exchanging the paths function, lightpaths are toggled from being primary paths to become backup paths while the corresponding backups are toggled to become primary paths. A hitless protection switching technique, which offers free switching between working and protection paths without any signal loss, has been introduced in [76, 77]. A similar hitless switching technique has been presented in [78] for protected passive optical network system. We suppose that the proposed scheme applies a hitless path protection switching technique, such as presented in [76, 77, 78], to exchange primary and backup paths.

To remove fragmentations, the proposed scheme reallocates lightpaths while they are in the backup state, where their reallocation does not affect the transmitted data. The reallocation process is supposed to be brief enough not to impair the 1+1 protection (quasi-1+1 protection). This allows us to achieve hitless defragmentation on both 1+1 paths without facing end of line situations when a spectrum jump is not allowed. Besides, the proposed scheme does not necessitate any additional network component, which is an advantage compared to using the

conventional scheme with designated primary and backup paths and applying spectrum retuning on primary paths.

We consider the defragmentation scheme with path exchanging to improve traffic admissibility in EONs with 1+1 path protection. We define a static path exchanging optimization problem that minimizes the spectrum fragmentation for a given set of lightpaths while limiting the number of combined exchanging and reallocation operations. We formulate the problem as an integer linear programming (ILP). We prove that the static spectrum reallocation decision problem for limited network operations is an NP-complete problem. For dynamic traffic setting, we present an approach that aims to remove the spectrum fragmentation while limiting the number of exchanging operations. A heuristic algorithm is introduced, since this problem is NP-complete; no efficient algorithm is found. On the other hand, the ILP approach to solve the NP-complete problem becomes impractical as the problem size increases. We evaluate the proposed scheme through different networks and varied settings. The results indicate that it reduces the bandwidth blocking probability in EONs and allows increased traffic loads compared to the conventional scheme, which uses designated primary and backup paths.

## 4.2 Proposed scheme

### 4.2.1 Path exchanging in 1+1 protection

To offer increased traffic load in resilient EONs, we propose a spectrum defragmentation scheme exchanging primary and backup paths in 1+1 path protection. For network resiliency, we consider a 1+1 path protection scenario to offer protection against link failures. With 1+1 path protection, each established signal is duplicated and both signals are transmitted to the destination through disjoint paths. This allows the receiver to select the incoming data from any of the two signals. Thus, if one path suffers link failure or is disconnected, the data reception is continued through the other path.

The proposed scheme considers that both paths of the 1+1 path protection can be alternately primary and backup paths. In order to perform spectrum

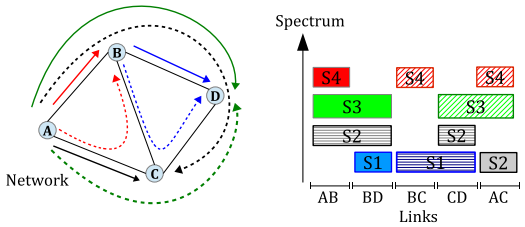


**(a)** Network and spectrum before defragmentation

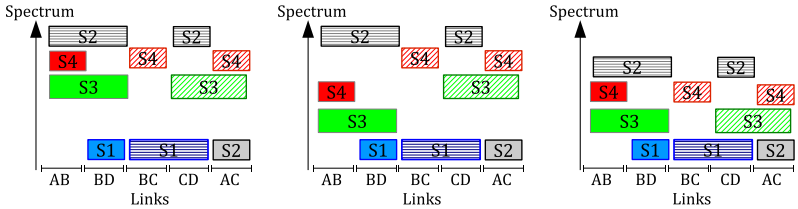


**(b)** Spectrum states using spectrum retuning on primary paths

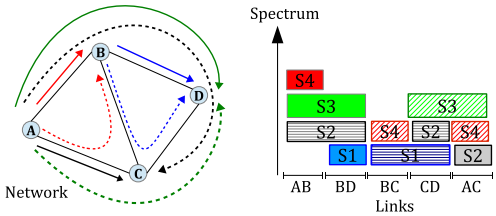


**(c)** Network and spectrum using path exchanges, backup reallocation without exchanging operation

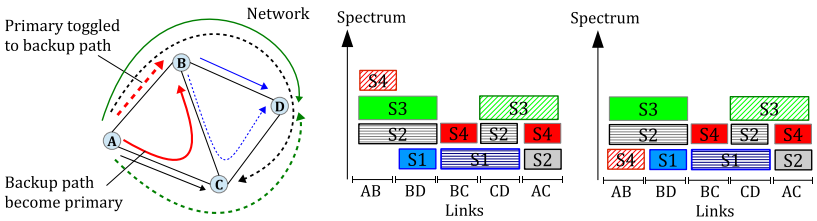


**(d)** Network and spectrum using path exchanges, path exchanging to reallocate initially primary path

**Figure 4.1:** Example of hitless defragmentation in 1+1 protection. Solid lines and plain boxes represent primary paths, dotted lines and hashed boxes represent backup paths.

defragmentation on primary paths, we simultaneously toggle them and their respective protection paths from primary to backup paths and from backup to primary paths respectively. Toggling a primary path to become a backup path changes its function from being the primary path through which the data is transmitted to become the backup path on standby. Thus, we exchange the function of the primary path to its backup path and vice versa. We allow backup paths on standby to be reallocated, for defragmentation, while the data is being transmitted through the primary path. We suppose that the period of release during the reallocation process is short enough to guarantee the 1+1 protection at almost every moment.

### 4.2.2 Hitless defragmentation with exchanging paths

The proposed scheme is able to achieve hitless defragmentation on 1+1 path protected networks without requiring any additional equipment. We take advantage of the availability of a by default alternate signal to reallocate lightpaths considering spectrum fragmentation. Since the data is being received through the primary paths, we can afford to reallocate the signals of backup paths during the defragmentation process without disrupting the data transmission. The defragmentation is performed without traffic disruption, provided that no failure occurs on a primary path while its corresponding backup path is being reallocated.

In terms of eliminating spectrum fragmentation, the advantage of the proposed scheme is to be able to reallocate both paths of the 1+1 protection for hitless defragmentation without restriction. With the conventional designated primary and backup paths where data from backup paths are used only if there is some impediment on the corresponding primary paths, only backup paths can be reallocated in a hitless defragmentation [65]. The ability to reallocate both primary and backup paths permits a flexible defragmentation that can be performed thoroughly.

Figure 4.1 illustrates the principle of the proposed defragmentation scheme with the function of exchanging the primary and backup paths in 1+1 protection network. Consider the network $ABCD$ with four active signals $S1 - S4$. The

network and its corresponding spectrum before proceeding to any defragmentation is presented in Fig. 4.1(a). The primary and backup paths of each signal are respectively represented by solid lines and dotted lines, and their corresponding spectrum by plain boxes and hatched boxes. On link $AB$, $S3$ and $S4$ are primary-path signals and $S2$ is a backup-path signal.

Figure 4.1(b) presents the network when the conventional designated primary and backup paths with spectrum retuning is used. After moving backup path $S2$, primary paths $S3$ and $S4$ are retuned. Then, the backup paths are reallocated using the first fit allocation. We can see that, in this particular example, spectrum retuning does not improve the spectrum fragmentation due to the end-of-line situation preventing $S4$ from being retuned over $S3$.

Figures 4.1(c) and 4.1(d) show the defragmentation process with the primary and backup paths exchanging. In Fig. 4.1(c), $S4$ signal through link $AC$, which is in the backup state is reallocated without path exchanging operation. Then, in Figures 4.1(d), $S4$ through link $AB$ is toggled to the backup state while its corresponding backup path on the 1+1 protection through links $AC$ and $BC$ becomes the primary path (see the network). While it is in the backup state, the lightpath $S4$ is reallocated to remove the spectrum fragmentation on link $AB$ (see the spectrum).

## 4.3 Static path exchanging optimization

### 4.3.1 Objective

We consider reducing the spectrum fragmentation from a static standing point. For a given set of lightpaths in an instance of initial fragmented spectrum state, we seek to rearrange their allocated spectrum to minimize the spectrum fragmentation in the returned target spectrum state. Since we intend to use the proposed path exchanging scheme for the transition between the initial state and the target state, we additionally set to limit the number of required network operations. In this setting, the network operations during the spectrum transition consist of the path exchanging operations to toggle primary lightpaths to the backup state and the operations of reallocating backup lightpaths.

We limit the number of network operations in order to avoid lengthy and repetitive defragmentation processes. In the case where the number of network operations is not considered, the optimization problem may return a configuration that requires an excessive number of lightpaths to be switched and/or moved. As a result the time to process the defragmentation increases compared to the lightpath inter-arrivals time. With more lightpath requests arriving before the defragmentation process is completed, this leads to additional bandwidth blocking, and reduced traffic admissibility. Additionally, an excessive number of network operations increase the operational expenditure as well. Therefore, we set to limit the number of network operations, which is minimized in an optimal scenario. We aim to select the solution that offers the minimum spectrum fragmentation with the lowest number of network operations.

### 4.3.2 Optimization problem

#### 4.3.2.1 Overview

To achieve the defined objective, the problem is approached as a static spectrum reallocation (SRR) problem, while considering to limit the number of network operations during the transition between the initial and target states. As such the problem can be viewed as two optimization problems: (i) The SSR problem that sets the target spectrum for a minimum fragmentation and (ii) the transition problem that minimizes the number of network operations required to reach the target state.

We note that with the target spectrum set by the SSR problem, the transition problem minimizes the number of network operations for that given instance of target spectrum state. It may happen that a different instance of target spectrum state, with similar spectrum fragmentation, requires a lower number of path exchanging operations and backup reallocation operations. To overcome this concern, we consider to define a problem formulation that combines the SSR problem to minimize the spectrum fragmentation and the transition problem to limit the network operations into a single problem. For the remaining of this paper, we refer to this problem as the static spectrum reallocation for limited network operations (SSR-LNO) problem.

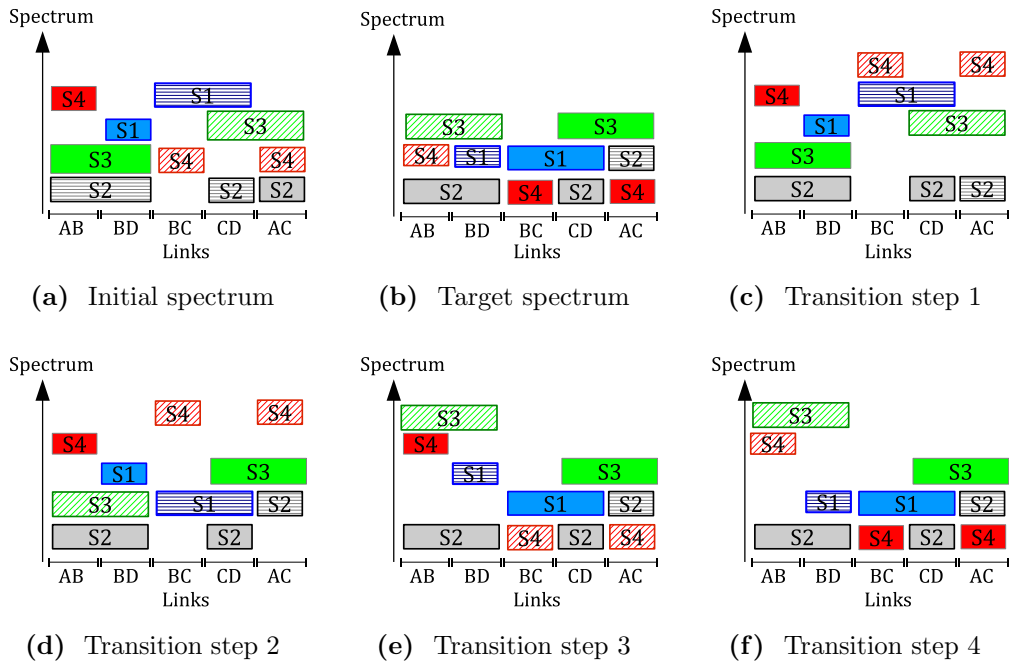


(a) Initial spectrum (b) Target spectrum (c) Transition step 1

(d) Transition step 2 (e) Transition step 3 (f) Transition step 4

**Figure 4.2:** Example of transition from initial to target spectrum. Plain boxes represent primary paths, and hashed boxes represent backup paths.

#### 4.3.2.2 Transition using path exchange

Solving the SSR-LNO problem returns the target spectrum state with reduced fragmentation and limited number of path exchanging and backup reallocation operations during the transition process. Suppose that a target spectrum state is given, we consider how the initial state is moved to the target state by applying the path exchanging scheme.

The path switching scheme allows the transition to be performed without data disruption. Nevertheless, as shown in the example of Fig. 4.2, it happens that some reallocation conflicts occur during the transition process. Figure 4.2(a) presents the initial spectrum consisting of four signals $S1, S2, S3$ and $S4$ and their respective primary and backup paths. The primary paths are represented by plain boxes and the backup paths by hashed boxes. Figure 4.2(b) presents a given target state to which we want to transit the spectrum. We can observe that the primary lightpaths of signals $S1$ and $S3$ cannot be moved to their intended

position before moving the other signal's primary lightpath.

To guarantee that all reallocation conflicts can be eluded during the transition process, we make sure that the spectrum can be rearranged to any returned target spectrum state with allowed reallocation moves. We formulate the SSR-LNO optimization problem with constraints to ensure that all intermediate states during the transition period are valid states. In other words, we identify all the transition steps, from the initial spectrum to the target spectrum.

Figure 4.2 (c)-(f) illustrate the steps of the transition using path exchanging. First, the backup lightpath of $S4$ is reallocated in order to free the spectrum slots that it was occupying. In parallel, we use the path exchanging to toggle the primary and backup paths of $S2$ (see Fig. 4.2(c)). Then, the backup lightpath $S2$, which was toggled in the previous step, is reallocated, while the path exchanging is used on $S3$ (see Fig. 4.2(d)). After that, we reallocate the backup lightpath $S3$ and toggle the primary and backup paths of $S1$ (see Fig. 4.2(e)). Then, the backup lightpath $S1$ is reallocated to its intended position, while the primary and backup paths of $S4$ are toggled (see Fig. 4.2(e)). Finally, the backup lightpaths $S3$ and $S4$ are reallocated (see Fig. 4.2(b)).

#### 4.3.2.3 Relation to two-dimensional bin packing problem

In terms of operation research, the SSR-LNO problem presents some similarities with the two-dimensional bin packing problem (2BP). In the 2BP, a set of $n$ rectangular items $j \in J = \{1, \cdots, n\}$ is given, with each having width $w_j$ and height $h_j$, and an unlimited number of finite identical rectangular bins, each of which has width $W$ and height $H$. The problem is to allocate all the items to a minimum number of bins [79]. The constraints restrict the items not to overlap, and their edges to be parallel to those of the bins. Additional constraints ensure that the items cannot be rotated or cut. With the SSR-LNO problem, each lightpath is seen as a rectangular item $j \in J = \{1, \cdots, n\}$, each of which has width $w_j$ equals to the number of routing hops and $h_j$ the number of required spectrum slots. The spectrum is considered as the first bin. The objective to minimize the spectrum fragmentation, formulated so as to minimize the highest

used spectrum index, corresponds to reducing the number of bins needed to fit all the items into the first one.

As the main different feature of the SSR-LNO problem compared with that of the 2BP problem, the route of a path is supposed to be fixed for the former. A lightpath is reallocated to different spectrum slots on the same links that it has been routed through. If we consider that the route of a path is translated to an item in the 2BP problem, each item has a fixed horizontal position, which changes the complexity of the problem. Furthermore, the SSR-LNO problem determines a target spectrum state to which the spectrum transits to, from a given initial spectrum state. The SSR-LNO problem ensures the feasibility of the path exchanging and reallocation operations during the transition steps. It also takes into consideration the number of network operations that are required to perform the transition.

### 4.3.3 Integer linear programming formulation for SSR-LNO problem

#### 4.3.3.1 Overview

We formulate the optimization problem to minimize the spectrum fragmentation while limiting the number of network operations as an integer linear programming (ILP) problem. We also set the objective function to minimize the highest used index, which is the highest spectrum slot used by a lightpath on any link of the network. Minimizing it limits the spectrum fragmentation since it pushes allocated lightpaths to the lower spectrum indexes (occupied spectrum indexes do not exceed the highest used index).

With the highest used index to be minimized in the objective function, several instances of spectrum rearrangement can yield the same minimum value. In order to choose the instance that requires the least number of network operations, we affix to this objective the secondary objective which is not a primary priority. The secondary objective is to select the instance that requires the least number of combined path exchanging and backup reallocation operations from the instances that yield the minimum highest used index. Note that the secondary objective can be defined to allow the selection of relaxed solutions with instances that require

low number of network operations given that they return the highest used index value close enough to the minimum value.

#### 4.3.3.2 Constraints

The constraints consist of the SSR constraints, which are the lightpath establishment, the spectrum consecutiveness and the slot capacity constraints, and the transition constraints to track and ensure the validity of the lightpath reallocation moves.

The lightpath establishment constraint ensures that all lightpaths are allocated. Each established lightpath is identified by its starting allocation index defined by the lowest spectrum slot index that it occupies. The spectrum consecutiveness is set so that lightpaths are allocated contiguous spectrum slot indexes. The spectrum slot capacity constraint prevents a spectrum slot index on a given link from being used by at more than one lightpath at the time. In other words, two lightpaths sharing a link cannot use the same spectrum slot index at the same time.

The transition constraints are introduced to track all lightpath reallocation moves during the transition period. They enforce the restrictions applying to the lightpath reallocation and the path exchanging operations, namely (i) a lightpath cannot be reallocated to slots used by another lightpath before the latter is reallocated, (ii) primary paths have to be toggled to the backup state before being reallocated, and (iii) the primary and backup lightpaths transmitting the same signal cannot be reallocated simultaneously.

#### 4.3.3.3 Notations

For the static defragmentation, the network's link capacity and spectrum state are given. All links ($e \in E$) are supposed to have the same capacity, which is the number of available spectrum slots $|F|$ per link, indexed from 0 to $|F| - 1$ as $F = \{0, \cdots, |F| - 1\}$. The initial spectrum state is represented by the set of lightpaths ($p \in P$) and their initial lightpath allocation indexes $f_p^{init}$. We refer to the set of path routed through link $e$ as $P_e$. The lightpaths' signal identifier $s(p)$ are also given; a primary lightpath and its backup lightpath share the same

signal identifier. The initial state of a lightpath $k_p^{init}$ is set to 1 for primary and 0 for backup. $n(p)$, which is a positive integer, represents the number of spectrum slots occupied by lightpath $p$ on links.

To ensure that the returned target state can be reached using the path exchanging scheme, we use on variables the step dimension $t$, in addition to the paths $p$ and indexes $f$, to follow the steps of the transition process. All constraints previously described must hold at each step $t$ of the transition process. The maximum number of steps $T$ is given as a parameter. We define $\tau = \{1, \cdots, T\}$ as the set of steps, $t = 0$ corresponds to the initial state, and $t = T$ corresponds to the returned state. During each step, either a swapping operation or a move operation can be performed on a given lightpath, but not both. On the other hand, multiple lightpaths can be considered in one step as long as the slot capacity and transition constraints hold. Note that the target state can be reached before running $T$ steps. It occurs if $T$ is larger than the number of required steps. As we limit the number of network operations with the second objective, the number of steps that it takes to reach the target state is not a concern as long as the transition constraints hold.

The used decision variables are described as follows. $U(t)$ is a positive integer defined as the highest spectrum slot occupied by any lightpath at step $t$. The binary variables $x_p^f(t)$ and $y_p^f(t)$ are used to identify respectively the starting allocation index $f$ of lightpath $p$ and a spectrum slot index $f$ allocated to lightpath $p$. $x_p^f(t)$ is set to 1 if $f$ is the lowest used index of lightpath $p$ at step $t$, and 0 otherwise. $y_p^f(t)$ is set to 1 if lightpath $p$ uses spectrum slot $f$ at step $t$, and 0 otherwise. Binary $k_p(t)$ represents the state of lightpath $p$ to indicate the primary or backup state at step $t$. It is put to 1 if lightpath $p$ is a primary lightpath and 0 if it is a backup one. The path exchanging operations are registered by $h_p(t)$, which is binary. $h_p(t)$ is set to 1 if primary lightpath $p$ is toggled to the backup state at the end of step $t$, and 0 otherwise. Recall that, while a primary lightpath is toggled to the backup state during a path exchanging operation, the corresponding backup is simultaneously toggled to the primary state. Therefore, counting the number of times a primary lightpath is toggled to backup is equivalent to counting the number of path exchanging operations. $m_p(t)$ is a binary

**Table 4.1:** Summary of notations for SSR-LNO formulation

| | |
|---|---|
| $E$: | Set of links. |
| $P$: | Set of lightpaths, $p \in P$. |
| $P_e$: | Set of paths using link $e$. |
| $F$: | Set of spectrum slot indexes, $f \in F$. |
| $\tau$: | Set of transition steps, $t \in \tau$. |
| $f_p^{init}$: | Initial allocation index of lightpath $p$. |
| $s(p)$: | Signal transmitted through lightpath $p$. |
| $k_p^{init}$: | Initial state of a lightpath $p$. 1 if primary, and 0 if backup. |
| $n(p)$ : | Number of spectrum slots required by lightpath $p$. |
| $U(t)$: | Highest used index on any link at step $t$ |
| $h_p(t)$: | Binary, 1 if lightpath $p$ toggles from primary to backup state at the end of step $t$, and 0 otherwise. |
| $x_p^f(t)$: | Binary, 1 if $f$ is the starting spectrum index allocated to lightpath $p$ at step $t$, and 0 otherwise. |
| $y_p^f(t)$: | Binary, 1 if lightpath $p$ uses spectrum slot index $f$ at step $t$, and 0 otherwise. |
| $m_p(t)$: | Binary, 1 if lightpath $p$ is reallocated at the end of step $t$, and 0 otherwise. |
| $k_p(t)$: | Binary, state of lightpath $p$ at step $t$. 1 if primary, and 0 if backup. |

to track whether lightpath $p$ is reallocated. It is activated to 1 if lightpath $p$ is reallocated during the transition between step $t$ and $t+1$, and 0 otherwise.

#### 4.3.3.4 SSR-LNO ILP problem

the ILP problem for the SSR-LNO is formulated as follows.

$$\min \quad U(T) \; + \; \epsilon \times \sum_{t=1}^{T} \sum_{p \in P} (h_p(t) + m_p(t)) \tag{4.0a}$$

Subject to

$$x_p^f(0) \; = \; 1 \;\; \forall \, p \in P, f = f_p^{init} \tag{4.0b}$$

$$k_p(0) \; = \; k_p^{init} \;\; \forall \, p \in P \tag{4.0c}$$

$$\sum_{f \in F} x_p^f(t) \; = \; 1 \;\; \forall \, p \in P, t \in \tau \tag{4.0d}$$

$$x_p^f(t) \; \leq \; y_p^{f'}(t) \; \forall p \in P, t \in \tau,$$
$$f \in \{0, \cdots, |F| - n(p)\}, f' \in \{f, \cdots, f + n(p) - 1\} \tag{4.0e}$$

$$x_p^f(t) \; = \; 0 \;\; \forall \, p \in P, t \in \tau,$$
$$f \; \in \; \{|F| - n(p) + 1, \cdots, |F| - 1\} \tag{4.0f}$$

$$\sum_{p \in P_e} y_p^f(t) \; \leq \; 1 \;\; \forall \, e \in E, f \in F, t \in \tau \tag{4.0g}$$

$$f \times y_p^f(t) \; \leq \; U(t) \; \forall \, p \in P, f \in F, t \in \tau \tag{4.0h}$$

$$|x_p^f(t) - x_p^f(t+1)| \; \leq \; m_p(t) \; \forall \, p \in P, f \in F, t \in \tau \backslash \{|\tau|\} \tag{4.0i}$$

$$y_p^f(t) + \sum_{p' \in P_e : p' \neq p} y_{p'}^f \; (t+1) \leq 1 \;\; \forall \, e \in E, p \in P_e,$$
$$f \in F, \;\; t \in \tau \backslash \{|\tau|\} \tag{4.0j}$$

$$k_p(t) + m_p(t) \; \leq \; 1 \; \forall \, p \in P, \;\; t \in \tau \tag{4.0k}$$

$$k_p(t+1) + m_p(t) \; \leq \; 1 \; \forall \, p \in P, \;\; t \in \tau \backslash \{|\tau|\} \tag{4.0l}$$

$$k_p(t) + k_{p'}(t) \; = \; 1 \; \forall \, t \in \tau \; p \in P, \;\; p' \in P, \;\; p' \neq p,$$
$$s(p') = s(p) \tag{4.0m}$$

$$k_p(t) - k_p(t+1) \; \leq \; h_p(t) \; \forall \, p \in P, t \in \tau \backslash \{|\tau|\} \tag{4.0n}$$

$$x_p^f(t), y_p^f(t) \; = \; \{0, 1\} \; \forall \, p \in P, \;\; f \in F, \;\; t \in \tau \tag{4.0o}$$

$$m_p(t), k_p(t), h_p(t) \; = \; \{0, 1\} \quad \forall \, p \in P, \;\; t \in \tau \tag{4.0p}$$

The objective to be minimized is the highest used index after the defragmentation $U(T)$. It is represented by Eq. (4.0a). The second part of Eq. (4.0a) is used to select the target spectrum that limits the number of network operations among solutions that have the same value for the first term of Eq. (4.0a).

It sums the number of path exchanging operations represented with $h_p(t) = 1$ when primary paths are toggled to the backup state and the number of backup reallocation operations represented with $m_p(t) = 1$. $\epsilon$ is selected small enough not to impair the first term of Eq. (4.0a). Eq. (4.0b) sets the initial spectrum. Eq. (4.0c) initializes the lightpaths' state, primary or backup. Eq. (4.0d) represents the lightpath establishment constraint, which ensures that, for each step $t$, lightpath $p$ is allocated and has a unique starting allocation index. The consecutiveness constraint is expressed by Eqs. (4.0e) and (4.0f). Eq. (4.0e) ensures that $y_p^{f'}(t)$ for each of the $(n(p)-1)$ spectrum slots $f'$ following the starting allocation index $f$ of lightpath $p$, for which $x_p^f(t)$ is equal to 1, is forced to 1. In other words, Eq. (4.0e) ensures that the $n(p)$ spectrum slots allocated to lightpath $p$ are consecutive from its starting allocation index $f$. Eq. (4.0f) ensures that there are at least $n(p)$ spectrum slots between the starting allocation index of lightpath $p$ and the last index of the spectrum. The highest used spectrum index, $U(t)$, is returned by Eq. (4.0h). It puts $U(t)$ equal to the highest spectrum index used by any path ($\max_{p \in P} f \times y_p^f(t)$) at step $t$.

Eqs. (4.0i) to (4.0m) represent the constraints to define and track the transition moves. Eq. (4.0i) tracks whether a lightpath is reallocated at step $t$. If lightpath $p$ is reallocated at step $t$, $m_p(t)$ is forced to 1. Any change between $x_p^f(t)$ and $x_p^f(t+1)$ forces $m_p(t)$ to 1 for Eq. (4.0i) to hold. In fact, for all $f \in F$, if either $x_p^f(t)$ or $x_p^f(t+1)$ is equal to 1, then the other term has to be equal to 1 for $m_p(t)$ to be equal to 0. This means, if lightpath $p$ is moved from or to the spectrum index $f$, then $m_p(t)$ is 1. Otherwise $m_p(t)$ is minimized to 0 by the second term of Eq. (4.0a).

Eq. (4.0j) forbids lightpaths to be reallocated to spectrum slots used by another lightpath with which it shares a link unless the latter has already been reallocated. In other words, we cannot reallocate a lightpath to spectrum slots used by another lightpath that is to be reallocated in the same step if they are not path disjoint. Eq. (4.0k) forbids primary lightpaths to be reallocated and Eq. (4.0l) makes sure that reallocated lightpaths cannot be toggled right away. Thus, they ensure that primary lightpaths are toggled to backup first before being reallocated and that reallocated lightpath cannot be used in a path exchanging operation during the same step. Eq. (4.0m) ensures that, while a lightpath is

in the primary state, the other lightpath of the 1+1 protection is in the backup state and vice-versa. Two lightpaths transmitting the same signal cannot be reallocated at the same time for data integrity.

Eq. (4.0n) detects the path exchanging operations by forcing $h_p(t)$ to 1 if lightpath $p$ is toggled from the primary state to the backup one. Otherwise, $h_p(t)$ is minimized to 0 due to the second term of the objective function. Finally Eqs. (4.0o)-(4.0p) define the binary variables.

### 4.3.4 NP-completeness

From the SSR-LNO problem, we define the SSR-LNO decision problem as:

**Definition 2** *Given a set of lightpaths $p \in P$, which can be in the primary or backup state and are initially allocated in the spectrum $F = \{0, \cdots, |F| - 1\}$, is it possible to reallocate all lightpaths with the highest used index at most $k$?*

**Theorem 2** *The SSR-LNO decision problem is NP-complete.*

**Proof 2** *The following proves Theorem 2.*

The SSR-LNO decision problem is NP, as we can verify whether an instance of the SSR-LNO decision problem has at most $k$ as the highest used index in polynomial time $O(1)$.

We show that the static lightpath establishment (SLE) problem, which is a known NP-complete problem [69], is reducible to the SSR-LNO decision problem. The SLE is defined as: is it possible to allocate a given set of lightpaths $p$ with the highest used index at most $h$ in a network $G(V, E)$?

First we construct an instance of the SSR-LNO decision problem from any instance of the SLE problem. An instance of the SLE problem consists of the set of lightpaths $p \in P$, the allocation index of the lightpaths $f_p$ and the threshold $h$ for the highest used index. An instance of the SSR-LNO decision problem is constructed with the following algorithm.

1. Define network $G'(V', E')$ with $|V'| = |V|$. Nodes $n', m' \in V'$ are connected by an edge in $G'(V', E')$ if and only if corresponding nodes $n, m \in V$ are connected by an edge in $G(V, E)$.

2. Define $P'$ as the set of lightpaths in $G'(V', E')$. For each lightpath $p \in P$, define a corresponding lightpath $q \in P'$ that follows the same routing path in $G'(V', E')$ as $p$ in $G(V, E)$. We set the state of all lightpaths $q \in P'$ as backup paths, which are reallocated without path exchanging.

3. Define the set of spectrum indexes $F' = \{0, \cdots, |F'|-1\}$ with $|F'| = 2 \times |P|$.

4. For each lightpath $q \in P'$:

i. Assign an initial allocation index $f_q^{'init}$ above $h$. The spectrum range of $F'$ is large enough to allocate all lightpaths above $h$. In the worse case scenario, where each spectrum index is used by a single lightpath, the required number of spectrum indexes is $|P| + h$ which is less than $|F'| = 2 \times |P|$, if $|P| > h$. The case with $|P| \leq h$ is trivial.

ii. Assign a reallocation index $f_q^{'final} = f_p$ , with $p \in P$ the lightpath corresponding to $q \in P'$, as defined in 2).

5. Set $k = h$.

The described algorithm has a polynomial complexity of $O(|P|)$. It transforms any SLE instance into an SSR-LNO instance. The input of the defined SSR-LNO instance is the initial lightpath allocation in the spectrum $F'$ and the output is the final lightpath allocation in the spectrum $F'$. Since all lightpaths are initialized as backup paths allocated with indexes above $h$, the transition from the initial state to the final state is performed in one transition step.

Consider that the SLE instance is a Yes instance. The highest used index is less or equal to $h$. By using the above described algorithm to define an SSR-LNO instance from any SLE instance, the highest used index by reallocated lightpaths in the SSR-LNO instance is the same as the highest used index by the lightpaths in the corresponding SLE instance. To each lightpath $q \in P'$, the algorithm assigns a reallocation index $f_q^{'final} = f_p$, where $f_p$ is the allocation index of the corresponding lightpath $p \in P$. With corresponding lightpaths $p \in P$ and $q \in P'$ having the same routing path, respectively in $G(V, E)$ and $G'(V', E')$, the spectrum layout after reallocation in the SSR-LNO instance is the same as the spectrum layout in the SLE instance. Therefore the highest used index by the

reallocated lightpaths in the SSR-LNO instance is less or equal to $k = h$, which means that the SSR-LNO instance is a Yes instance.

Conversely, if the SSR-LNO instance is a Yes instance then the SLE instance is a Yes instance. Since $k$ is defined to be equal to $h$ as discussed above, the highest used index by the reallocated lightpaths in the SSR-LNO instance is the same as the highest used index by the lightpaths in the SLE instance.

We have confirmed that using the described transformation, if the SLE instance is a Yes instance, then the corresponding SSR-LNO instance is a Yes instance, and conversely. This proves that the SLE decision problem, a known NP-complete problem, is polynomial time reducible to the SSR-LNO decision problem. Thus, the SSR-LNO decision problem is NP-complete. ■

Note that the SSR-LNO instance defined by the transformation algorithm is made of only backup paths. For an instance with primary and backup paths in the 1+1 protection, we consider network $G''(V'', E'')$, which is an extension of network $G'(V', E')$, where $V'' = V'$, with an edge $(s, d)$ added to connect source $s \in V'$ and destination $d \in V'$, for all source/destination pairs. The backup paths $q \in P'$ are defined in the same way as the transformation algorithm. For each lightpath $q \in P'$, its corresponding primary path is routed through the added edge between its source $s$ and destination $d$, and is allocated using first-fit allocation. Edge $(s, d) \in E''$ is used only by the primary paths from source $s$ to destination $d$. Since the first-fit allocation is used, edge $(s, d) \in E''$ does not present any fragmentation. As a result, the primary lightpaths are not touched during the defragmentation, and the highest spectrum index used by a primary lightpath is at most $h$. If the backup lightpaths can be reallocated with the highest used index being at most $h$, then the SSR-LNO instance is a Yes instance.

# 4. PATH EXCHANGING SCHEME IN 1+1 PROTECTED ELASTIC OPTICAL NETWORKS

# Chapter 5

# Path exchanging Scheme for dynamic traffic

## 5.1 Defragmentation approach using path exchanging scheme

### 5.1.1 Overview

With the aim to allow maximum traffic load in 1+1 path protected EONs, the proposed paths exchanging scheme is applied. It reduces the blocking probability by minimizing the spectrum fragmentation. The way the proposed scheme is applied depends on the traffic pattern. With static traffic loads, the spectrum state does not change often overtime, but with dynamic traffic loads, the spectrum is in constant evolution. In the case of static traffic load, spectrum fragmentation can be avoided by network planning, and the optimization problem is used in the rare occasions where changes are needed including the cases of network extensions and reconfigurations. On the other hand, for dynamic traffic loads where lightpaths can be added or removed at any moment, the spectrum has to be defragmented frequently in order to avoid requests being blocked due to fragmentation. In the following, we focus on dynamic traffic loads.

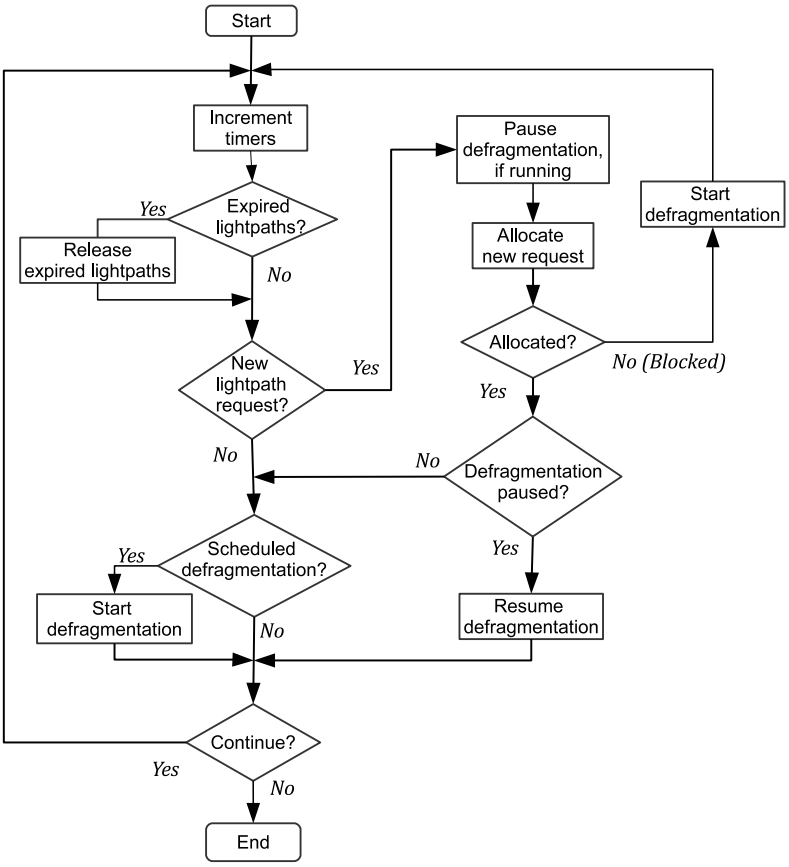


**Figure 5.1:** Flowchart of dynamic approach.

### 5.1.2 Dynamic spectrum defragmentation

In our approach to tackle spectrum fragmentation in EONs with dynamic traffic, we suppose that the network can receive a lightpath request at any moment and that allocated lightpaths are active for the requested time periods. The spectrum defragmentation process is triggered at a regular time interval in addition to being automatically triggered whenever a request is blocked. We select to use scheduled defragmentation in a proactive way to prevent blocked requests and limit the processing cost.

It would be preferable to repeat the defragmentation process as much as possible; however that comes with a cost in processing. The scheduled defragmentation offers a compromise as the period between defragmentation processes can be suitably set. Nevertheless, it may happen that between defragmentation processes

the cumulative fragmentation causes requests to be blocked. To avoid prolonged blocking until the next scheduled defragmentation, we elect to trigger the defragmentation process whenever a blocking occurs. The overall process of our approach is presented in Fig. 5.1.

### 5.1.3 Defragmentation process

When the defragmentation process is triggered, the spectrum state at that instant is taken as static and used as an input instance to the SSR-LNO problem. Solving the SSR-LNO problem returns the target spectrum state which can be reached using the path exchanging scheme. Then, the spectrum is reconfigured to the target spectrum state, to remove the spectrum fragmentation, following the transition steps. Ideally, the SSR-LNO problem is solved and the transition is performed before a new lightpath request arrives. However, in reality the SSR-LNO problem requires some computation time, particularly if the ILP approach is used. In addition, it is likely that request arrivals occur during the transition period.

Nevertheless, the overall process described in the previous section allows us to tackle the dynamic defragmentation, granted that the SSR-LNO is solved in a practical time. The defragmentation process is interrupted by request arrivals, and otherwise it proceeds as supposed. Lightpath removals do not affect the defragmentation process as removed lightpaths are just ignored during the transition steps. Since the SSR-LNO decision problem is NP-complete, which means the ILP solving time exponentially increases with the network scale, we introduce a heuristic algorithm for large networks with dynamic traffic.

### 5.1.4 Heuristic algorithm

We introduce a heuristic algorithm for the dynamic spectrum defragmentation. The input spectrum is the state at the moment the defragmentation process is triggered. As the SSR-LNO problem can be related to the 2BP problem, one may consider some heuristic algorithms for the 2BP problem [79, 80, 81] as candidates for the SSR-LNO problem. However, due to the differences between the two problems those heuristics are not suitable. For example, the most common

approach for the 2BP problem, the bottom-up left-justified approach [80], which places an item into the lowest possible left-justified location, cannot be applied to the SSR-LNO problem due to lightpaths using a fixed set of links. Another limitation is that the SSR-LNO has to consider moving certain lightpaths before reallocating other lightpaths at their occupied spectrum slots, which is not considered by the 2BP problem.

On the other hand, certain aspects from heuristics for the 2BP problem are considered in our heuristic. The objective set in [80] to minimize the height achieved by any item is the same as our objective to minimize the highest spectrum index used by any lightpath. The best fit strategy, which aims to minimize the unused space after an item is packed [79], is similar to our strategy to use the exact-fit allocation. To finish our heuristic uses a two-phase approach, which is used in 2BP heuristics [81].

#### 5.1.4.1 Mixed primary and backup path algorithm

Our introduced heuristic algorithm for dynamic spectrum defragmentation, which is called a mixed primary and backup (MPB) algorithm (See algorithm 2), consists of three steps: (i) sort all lightpaths, both primary and backup paths, in a single list, according to a policy, (ii) proceed to the first defragmentation stage by reallocating lightpaths following the sorted list, and (iii) refine the defragmentation by reallocating lightpaths that can be pushed further down.

In the first step, we sort all lightpaths in a single list, regardless of their initial state (primary or backup) following the selected sorting policy. Since, to reallocate a lightpath in the primary state, we first toggle it to the backup state while its backup is toggled to the primary state, the state of a lightpath may change during the defragmentation process. We consider the path length and the request size as sorting parameters. The length of a path, primary or backup, is the number of link hops on the path. It may be different for corresponding primary and backup paths. A request size represents the number of spectrum slots used by a lightpath. Using these parameters we introduce two sorting policies; the longest path first and the largest slot block first. The slot block area is the product of the path length by the request size.

In the second step, we perform the first stage of defragmentation. Following the sorted list, we reallocate lightpaths to the lower spectrum indexes. At each iteration, we select several lightpaths that can be considered simultaneously. The first selected lightpath is the top of the list. The other lightpaths, which has to satisfy the simultaneous reallocation conditions described as follows, are selected through the list. All the selected lightpaths must be link disjoint and transmitting different signals; we cannot select two lightpaths sharing any link or the primary and backup lightpaths of the same 1+1 protection to avoid reallocation conflict. Once the candidate lightpaths are selected, we reallocate them using the exact-fit policy. The primary lightpaths are toggled to the backup state before reallocation. We refer to the exact-fit allocation policy when we attempt to allocate a lightpath to a free spectrum slot block consisting of exactly the same number of consecutive spectrum slot indexes as the number of spectrum slots required by the lightpath. If there is no such block, we use the first-fit allocation policy. When a lightpath cannot be reallocated to a lower allocation index, it remains at its current allocation index. After that, the selected lightpaths are removed from the list. We repeat the same procedure until all lightpaths are selected.

During the second step of the algorithm, once a lightpath has been selected for reallocation, it is not be revisited. For instance, when a short lightpath previously allocated to a relatively low spectrum index is reallocated, a longer lightpath, which was selected earlier than the shorter one and was reallocated above the spectrum indexes that were previously used by the short lightpath, is not reconsidered. If the spectrum slots freed from reallocating the short lightpath concatenate with some empty slots, the resulting slot block could be used by the longer lightpath. We take this possibility into account with the third step of the algorithm.

In the third step, we refine the spectrum defragmentation by finding the lightpaths that can still be reallocated to lower spectrum indexes. For that, our approach selects lightpaths to be reallocated starting from the ones allocated at the lowest spectrum index. We initialize a pointer at index 0. Then, after each reallocation iteration, we increment the pointer by 1 and select the lightpaths to be considered for reallocation as the ones allocated at the pointed index. We repeat until the highest allocation index is reached. In other words, we reallocate

**Algorithm 2:** Mixed primary and backup paths defragmentation.

**Input**: Spectrum, active signals

**Output**: Defragmented spectrum

**Step 1:** Sort all lightpaths according to policy

**Step 2:** First stage defragmentation

2.1: Select the lightpath at the top of the sorted list,

2.2: Select other lightpaths that can be reallocated in parallel with the first selected lightpath, following the sorted list,

2.3: Reallocate selected lightpaths using the exact-fit policy. If primary path toggle first,

2.4: Remove selected lightpaths from the list,

2.5: Repeat from 2.1, until all lightpath are selected.

**Step 3:** Refining defragmentation

3.1: Initialize pointer at index 0,

3.2: Increment pointer,

3.3: Reallocate selected lightpaths $p$ using the exact-fit policy. If $p$ is a primary, then first toggle $p$.

3.3: Repeat from 3.2, until the highest allocation index is reached.

the lightpaths allocated on lower spectrum indexes first so that the lightpaths allocated on higher spectrum indexes can be reallocated to the vacant spectrum that they left behind. We still use the exact-fit allocation policy in this step and we reallocate a lightpath only to spectrum indexes lower than its currently occupied ones.

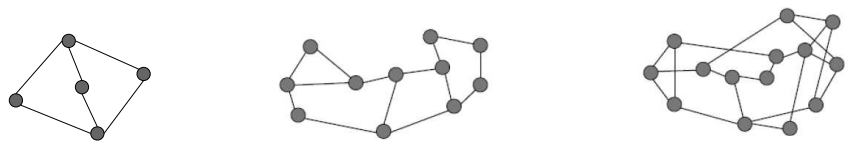

**(a)** Five-node **(b)** Abilene **(c)** NSFNet

**Figure 5.2:** Simulation networks.

#### 5.1.4.2 Time and spatial complexity

We analyze the time and spatial complexity of the MPB heuristic algorithm. The maximum number of active lightpaths is bounded by the spectrum capacity, which is the total available spectrum slots through all links $N = |F| \times |E|$. In term of time complexity, step 1 of the algorithm is performed in $O(N \log N)$, and both steps 2 and 3 are performed in $O(N \times |F|)$. In each of steps 2 and 3, each lightpath is reallocated at most once and each reallocation process requires $O(|F|)$, which is the time to find the reallocation spectrum slots. The overall time complexity of the algorithm is $O(N(|F| + \log N))$.

For the spatial complexity, during each of its steps, the algorithm saves the spectrum state with the informations related to the active lightpaths including starting allocation indexes and required slots. From one step to the next, the spectrum state and active lightpaths are updated using the same allocated memory. Since saving both the spectrum state and the active lightpaths requires each $O(N)$ memory space, the memory requirement of the algorithm is $O(N)$.

## 5.2 Results and discussions

### 5.2.1 Simulation settings

To assess the allowable traffic load, we evaluate the bandwidth blocking probabilities of the proposed path exchanging scheme through simulation. The following assumptions are considered for the purpose of simulation. Lightpaths are initially established using the first-fit allocation policy for all evaluated approaches. If not specified, the proposed scheme uses the introduced MPB heuristic algorithm, and

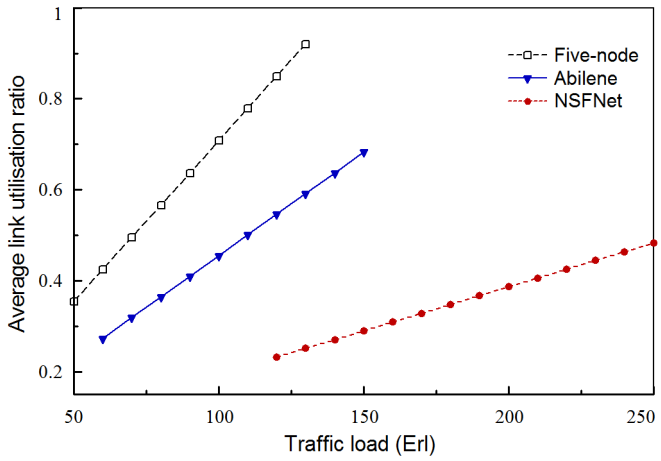


**Figure 5.3:** Average link utilisation versus traffic load (Erl).

the path length sorting policy is used by the default. The connection requests are generated randomly based on a Poisson distribution process ($\lambda$) and the holding time of connection requests follows an exponential distribution ($H = 1/\mu$). The traffic load is given in Erlang by $\rho = \lambda \times H$. The source and destination of each request are supposed to be randomly independent from the previous ones and the number of requested slot blocks per lightpath is uniformly distributed. The routing for the primary and backup paths of each lightpath is supposed to be given in advance, since we focus on the defragmentation performance. The routes are fixed for each source and destination pair. They are determined in order to minimize the maximum traffic passing through any given link in the network [66]. We run the simulation for 200 different seeds, with each of which 10000 lightpath connection requests are generated. For the bandwidth blocking probability, simulation results are obtained with a 95% confidence interval that is not greater than 5% of the reported average results.

Figure 5.3 presents the average link utilization, presented as a function of the offered load, $U(\rho)$, given by the following equation.

$$U(\rho) = \frac{\rho \times \text{Avg. route hops} \times \text{Avg. requested slots}}{|F| \times |E|} \tag{5.1}$$

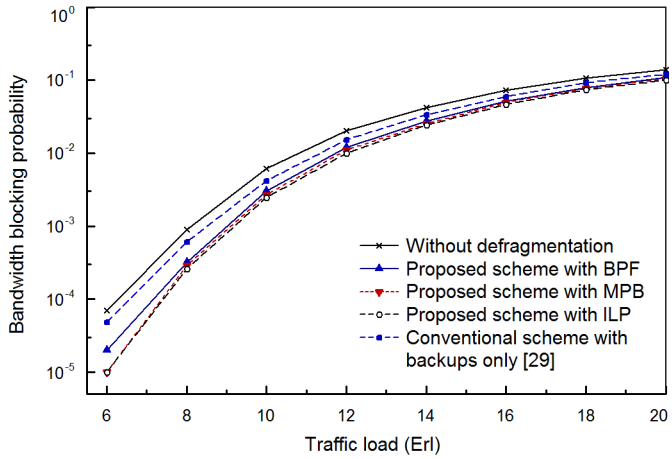


**Figure 5.4:** Comparison of bandwidth blocking probabilities.

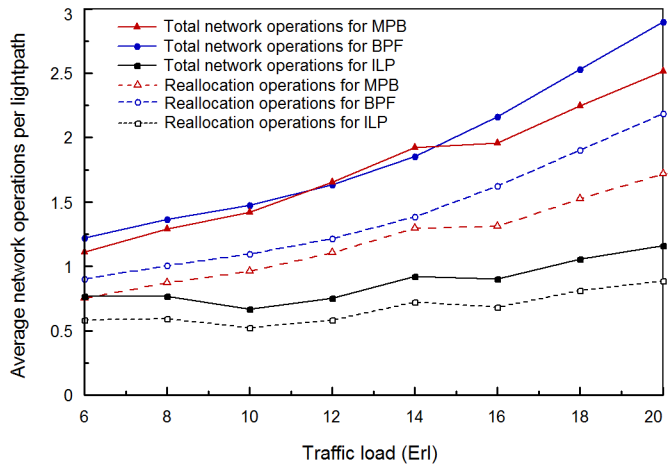


**Figure 5.5:** Number of network operations comparison. The total number of network operations consists of the number of reallocation operations and the number of path exchanging operations.

### 5.2.2 Heuristic performance comparison with ILP results

#### 5.2.2.1 Bandwidth blocking performance

To assert the efficiency of the introduced MPB defragmentation algorithm, we compare its performances against the ones obtained using the ILP approach. We also compare the results of the MPB algorithm with another heuristic algorithm where we elect to reallocate the backup paths first. The backup paths first (BPF) algorithm sorts the lightpaths in the primary state and in the backup state on separate lists. Then, it reallocates all the lightpaths that are in the backup state before considering the list of lightpaths in the primary state. Since the running time to solve the ILP problem increases exponentially with the network scale, we have limited its simulation on the five-node network (see Fig.5.2(a)), where we set the link capacity to 24 slots and the maximum request size for a lightpath to four slot blocks. We compute the ILP with the CPLEX solver [74].

Figure 5.4 presents the obtained results in terms of bandwidth blocking probability. We observe that the MPB algorithm presents results that are similar to the ones obtained using the ILP approach. As a result, when the path exchanging scheme is applied, the MPB algorithm can be used instead of the ILP approach which necessitates exponential solving time for large networks. The BPF algorithm yields comparable results, with a slight increase of the number of blocked requests. With the primary lightpaths not moved during the reallocation of the backup lightpaths, the BPF approach has less spectrum flexibility. The bandwidth blocking performances presented in Fig. 5.4 indicates that the proposed path exchanging scheme is efficient in terms of defragmentation capability. Fig. 5.4 also show that the proposed scheme outperforms the conventional scheme used in [65], where only the backup path are included in the defragmentation process.

#### 5.2.2.2 Number of network operations

The heuristic algorithms lead to an increase in the number of network operations required during the defragmentation process, as illustrated in Fig. 5.5. Figure 5.5 shows that the algorithms cannot match the ILP approach when it comes to the number of network operations. In fact, this was to be expected since we have

formulated the ILP approach to choose the solution with the lowest number of network operation for each instance (recall Eq. (4.0a)), which is not the case for the heuristic algorithms.

The MPB algorithm shows a lower number of reallocation operations, and a slightly lower number of network operations than the BPF algorithm. The BPF algorithm compensates its higher number of reallocation operations by offering lower number of exchanging operations. With the backup paths reallocated first, the number of required path exchanging operations is limited to the number of primary paths that are to be reallocated. In the case of the MPB algorithm, primary paths are toggled to the backup state before reallocation with their corresponding backup paths toggled to the primary state. As a result, lightpaths that were toggled to the primary state, are toggled back to the backup state when it is their turn to be reallocated. Therefore, the MPB algorithm requires more path exchanging operations. The advantage of the MPB algorithm resides in the fact that the sorting policy is selected to minimize the number of reallocation operations, which corresponds to the number of times the 1+1 protection is breached.

### 5.2.3 Performance comparison with conventional scheme

We compare the proposed path exchanging scheme to the conventional scheme with designated primary and backup paths using networks presented in Fig. 5.2. The Abilene and the NSFNet networks, are commonly used for backbone simulations [73]. The channel spacing and the total number of spectrum sub-carrier slots per channel are considered as 12.5 GHz and 400, respectively. The maximum request size is set to 16.

We consider the effect of the processing speed on the performance of the proposed scheme and the conventional one with spectrum retuning. In the proposed path exchanging scheme, we suppose it takes $\beta$ [time unit] to reallocate a lightpath including the toggling operation. In the conventional scheme with the spectrum retuning, the time needed to retune a lightpath from its initial index to its destination index is estimated as the product $t_{ret} = \alpha \times s + \delta$; with $\alpha$ being the sweep time per slot, $s$ the number of moved slots and $\delta$ the operational time,

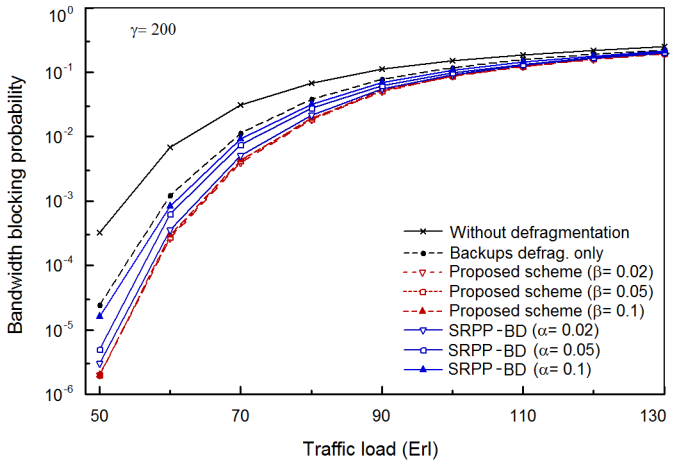


**(a)** Five-node

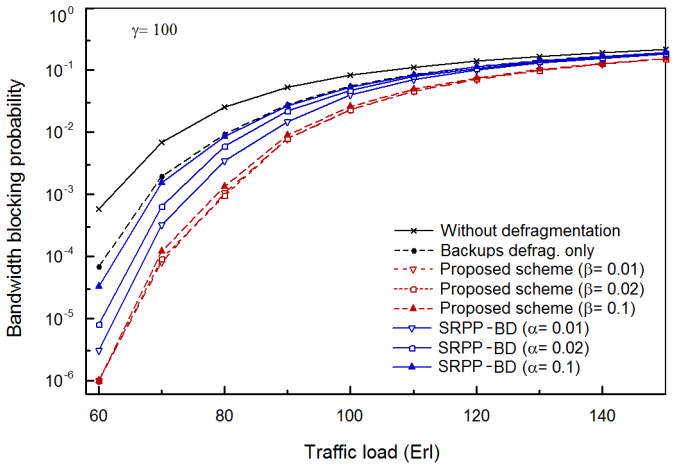


**(b)** Abilene

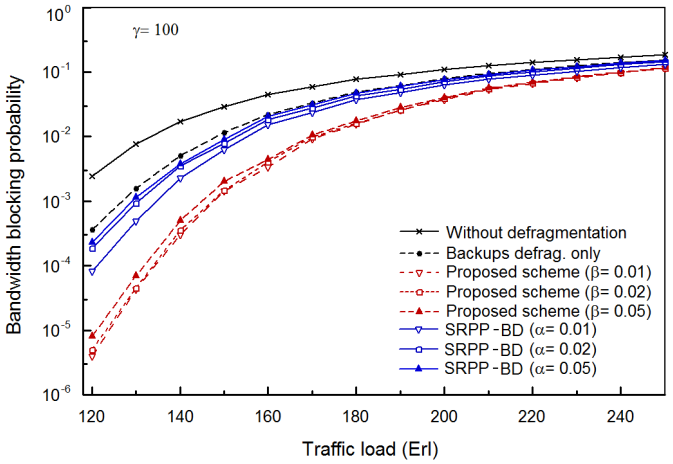


**(c)** NSFNet

**Figure 5.6:** Effect of the processing speed on the defragmentation schemes.

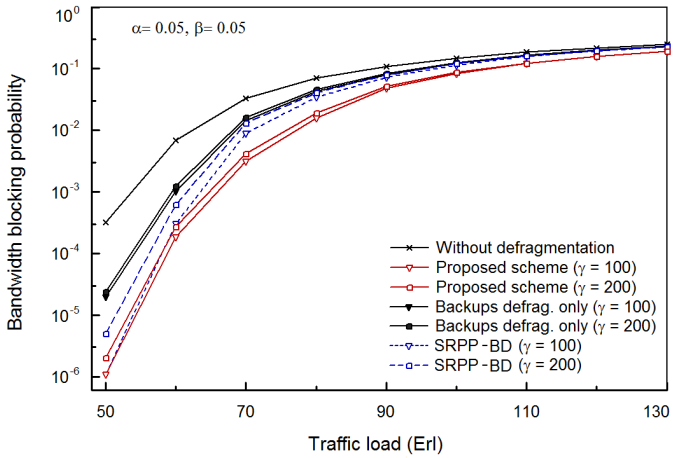


**(a)** Five-node

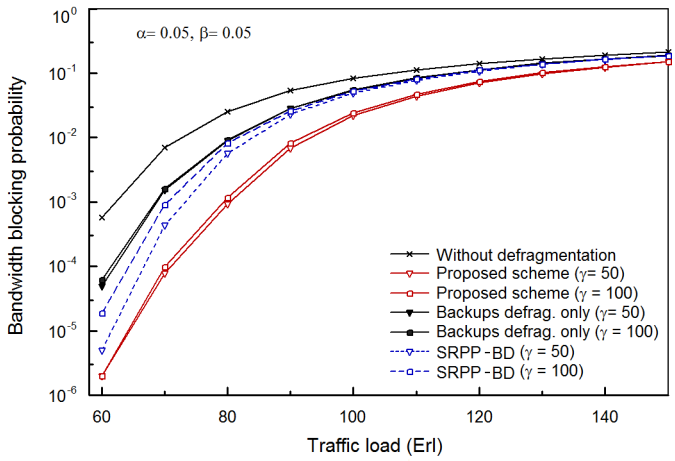


**(b)** Abilene

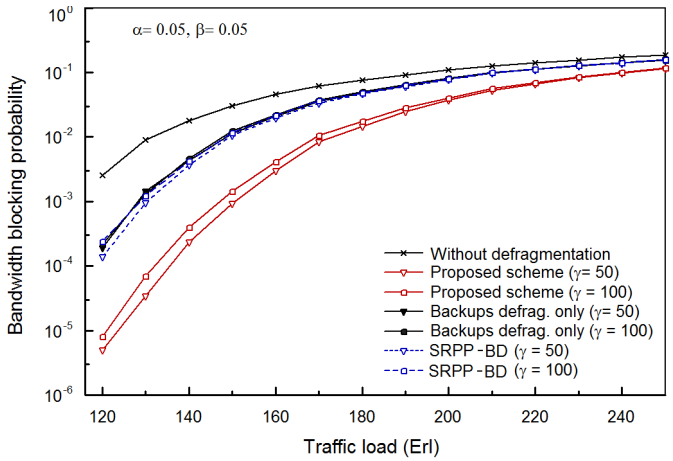


**(c)** NSFNet

**Figure 5.7:** Impact of the interval time between defragmentation.

the time needed for synchronisation and activation, which is neglected in this evaluation. We consider $\alpha$ varying from 0.005 [time unit] to 0.5 [time unit] sweep time per slot, which correspond to sweeping rates ranging from 1 to 100 ms/2.5 GHz in a 12.5 GHz grid [46] for 1 sec as time unit.

Figures 5.6 and 5.7 show the bandwidth blocking probabilities of the proposed path exchanging scheme compared to the conventional scheme using designated primary and backup paths. For the conventional scheme we consider two cases, (i) the approach presented in [65], where only backup paths are defragmented by reallocation (Backup defrag. only), and (ii) spectrum retuning is used to defragment the primary paths before the reallocation of the backup-path (SRPP-BD). Figures 5.6 and 5.7 present the simulation results on the three considered networks for varied $\alpha, \beta$, and $\gamma$, where $\gamma$ denotes the interval time between scheduled defragmentations. The results confirm that the proposed scheme outperforms the two cases of the conventional scheme. By allowing spectrum reallocation on both 1+1 protection paths, the proposed path exchanging scheme defragments the spectrum more thoroughly than the conventional one. It reduces the bandwidth blocking probability up to 75% and increases the allowable traffic to around 10% at 0.01 blocking ratio.

In Fig. 5.6, we observe that the processing speed has little effect on the performances of the proposed path exchanging scheme. This is because the defragmentation process requires only $\beta$ time per reallocated path and the maximum $\beta$ is relatively short compared to the request inter-arrival time. On the other hand, the performances of the conventional scheme with spectrum retuning are strongly correlated with the processing speed. The time needed to retune a lightpath also depends on the number of moved slots. When the retuning is fast enough, it is negligible and the conventional scheme with spectrum retuning shows blocking performances close to those of the proposed scheme. However, with slower retuning speed, the defragmentation performances are affected, and the blocking ratio tends closer to that when only the backup paths are defragmentated.

In Fig. 5.7, the effects of the defragmentation frequency on the performance of both proposed and conventional schemes are presented. We observe that the best performances are realized when the defragmentation process is triggered more frequently, i.e., when $\gamma$ is small. Nonetheless, the proposed scheme presents, for the

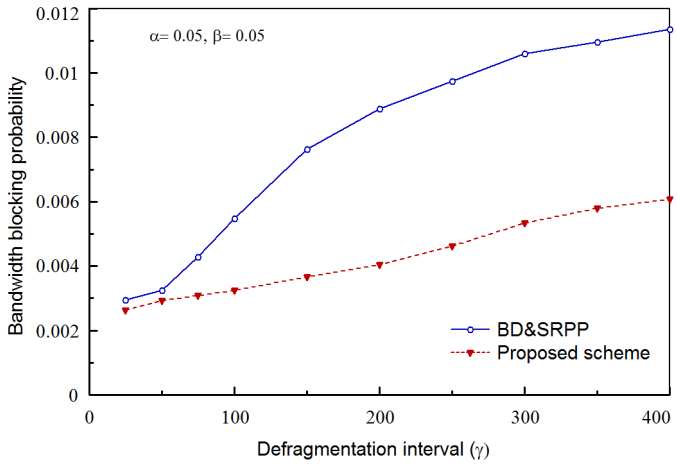


**Figure 5.8:** Bandwidth blocking probability versus defragmentation interval ($\gamma$).

case that the defragmentation process is triggered less frequently, blocking performances that are close to the best performances. In comparison, the blocking performances of the conventional scheme, for the case that the defragmentation process is triggered less frequently, are degraded. This is confirmed by Fig. 5.8 where the bandwidth blocking probability is represented in terms of the defragmentation interval, $\gamma$, for $\alpha = \beta = 0.05$ and a traffic load of 70 erl in the five-node network. Fig. 5.8 shows, for the path exchanging scheme, a slow but steady increase of the bandwidth blocking probability as $\gamma$ increases. We note a slightly faster increase rate when $\gamma$ is between 200 and 300. On the other hand, for the conventional SRPP-BD, the increase rate is slow for $\gamma$ lower than 50 and larger than 300. However between those two values, the bandwidth blocking probability rise considerably. In short, Fig. 5.8 shows that the blocking performance of the path exchanging scheme will be similar for $\gamma$ lower than 200, and for $\gamma$ lower than 50 in the case of the conventional SRPP-BD. In both cases, the effectiveness of the defragmentation is reduced for $\gamma$ superior to 300.

In general, the processing speed and the defragmentation frequency have a combined effect on the blocking performances. The best performances are achieved with high processing speed and frequent defragmentation process. However, this has the trade-off of requiring high-end equipment to achieve top processing speed, and increased network operations for frequent defragmentation process.

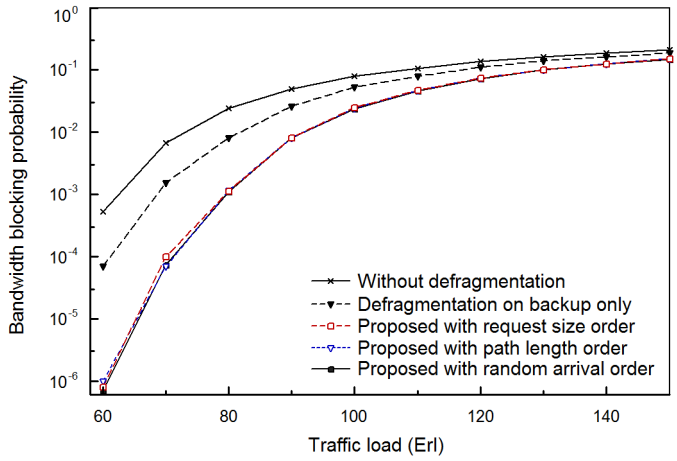


**(a)** Bandwidth blocking performance.

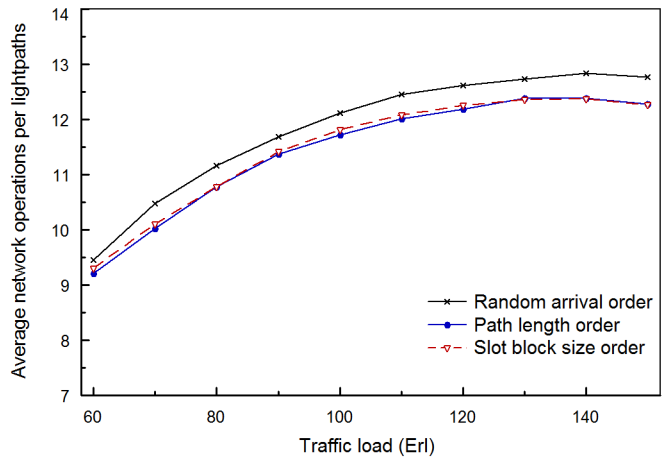


**(b)** Average number of network operations.

**Figure 5.9:** Performances of path exchanging for different sorting policies (Abilene).

When the processing speed is limited and/or the defragmentation frequency is reduced, the proposed scheme outperforms the conventional one.

### 5.2.4 Effect of sorting policy

We investigate the effect of using different sorting policies in the defragmentation process of the path exchanging scheme. The obtained results are presented in Fig. 5.9. We observe that the different sorting policies considered, namely path length, occupied slot blocks and request arrival order for random consideration, have similar performances in terms of allowable traffic (see Fig. 5.9(a)). We observe that, the required number of network operations increases with the traffic load, before reaching a saturation point. Then, it starts to decrease (see Fig. 5.9(b)). For higher traffic loads, the spectrum becomes more and more occupied. As a result, we witness the saturation and then the decrease of the number of reallocation possibilities. When comparing the sorting policies, the random sorting by request arrival order uses the highest number of operations. The sorting policy by path length order offers the lowest number of network operations with a slight advantage compared to the sorting policy by occupied slot block size order. Reallocating the longer paths first reduces the spectrum availability for subsequent reallocation. This effect is balanced when the sorting is performed by occupied slot block size due to the requested bandwidth size factor.

### 5.2.5 Effect of allocation delay

The results discussed up to this point are obtained with the consideration that no delay is allowed during the allocation of new requests. All blocked requests were automatically discarded. In the following, we relax that constraint by allowing a delay threshold during which the spectrum can be defragmented before retrying to allocate a waiting request.

Figure 5.10 shows the blocking performances depending on the delay threshold. The performances are overall improved (see Fig. 5.10(a)). The observations previously made when no delay was allowed still hold, namely (i) the proposed scheme outperforms the conventional one, (ii) the performances depend on how frequently the defragmentation are performed, and (iii) the conventional scheme

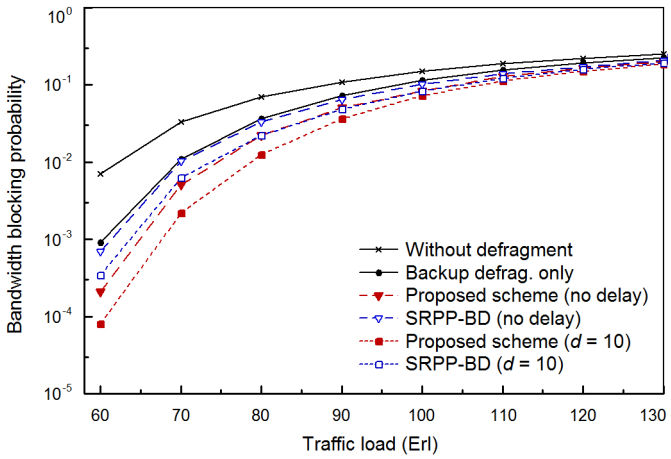


**(a)** Bandwidth blocking performance.

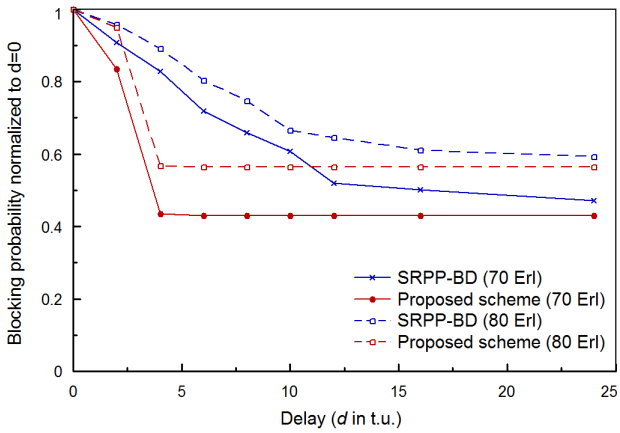


**(b)** Effect of delay time on blocking performance.

**Figure 5.10:** Impact of allowed allocation delay ($d$ in time unit) on defragmentation schemes (Five-node network).

with spectrum retuning depends on the processing speed while the proposed scheme is mostly affected. Additionally the proposed path exchanging tends to reach maximum improvement much faster (see Fig. 5.10(b)).

## 5.3 Summary

Sections 4 and 5 presented a defragmentation scheme using primary and backup paths exchanging in 1+1 path protected EONs to improve traffic admissibility. The presented scheme toggles the function of the lightpaths in a 1+1 path protection from the primary state to the backup state alternately to allow initially primary lightpaths to be reallocated for defragmentation purpose. The path exchanging scheme offers a hitless defragmentation of the spectrum by applying hitless path protection switching. An optimization problem of the static spectrum reallocation with limited network operations (SSR-LNO), which minimizes the spectrum fragmentation, have been defined and formulated as an ILP problem. The SSR-LNO decision problem has been proven to be NP-complete. A spectrum defragmentation approach for dynamic EONs has presented, and a heuristic algorithm tractable for large networks introduced. The simulation results suggest that the introduced heuristic algorithm offers blocking performances comparable to the ones obtained using the ILP approach. The proposed path exchanging scheme outperforms the conventional scheme with designated primary and backup paths, with up to 10% additional admissible traffic when the processing speed is considered.

# Chapter 6

# Conclusions and future works

## 6.1 Conclusions

This thesis considers hitless defragmentation in order to increase the allowable traffic in EONs. Two schemes were presented: (i) a route partitioning scheme for default EONs, where spectrum jump is not allowed, and (ii) a path exchanging scheme in 1+1 protected EONs, where backup paths can be reallocated without disrupting the traffic.

First, the route partitioning scheme , which uses first-last fit allocation, increases the possibilities of lightpath retuning by avoiding the retuning interference among lightpaths. The use of first-last fit reduces the number of needed retuning operations and the retuning time, while the route partitioning furthers the possibility of retuning by avoiding end-of-line situations. The route partitioning problem was defined as an optimization problem and an ILP problem was formulated to solve it. The route partitioning problem was proven to be NP-hard, and a heuristic algorithm was presented for large networks, where the ILP to represent the route partitioning is not tractable. The numerical results showed that the proposed scheme offers reduced bandwidth blocking probability with limited retuning speed. Furthermore, the proposed scheme allows up to 10% more traffic compared to the conventional hitless defragmentation.

Second, the path exchanging scheme allows primary and backup paths exchanging in 1+1 path protected EONs to improve traffic admissibility. The scheme toggles the function of the lightpaths in a 1+1 path protection from the

primary state to the backup state alternately to allow initially primary lightpaths to be reallocated for defragmentation purpose. The path exchanging scheme offers a hitless defragmentation of the spectrum by applying hitless path protection switching. An optimization problem of the static spectrum reallocation with limited network operations (SSR-LNO), which minimizes the spectrum fragmentation, have been defined and formulated as an ILP problem. The SSR-LNO decision problem has been proven to be NP-complete. A spectrum defragmentation approach for dynamic EONs has presented, and a heuristic algorithm tractable for large networks introduced. The simulation results suggest that the introduced heuristic algorithm offers blocking performances comparable to the ones obtained using the ILP approach. The proposed path exchanging scheme outperforms the conventional scheme with designated primary and backup paths, with up to 10% additional admissible traffic when the processing speed is considered.

## 6.2 Future works

This thesis presented hitless defragmentation schemes, which are positioned for implementation in future EONs. In order to implement the schemes, several steps are to be taken. The presented work focuses mainly on overcoming the spectrum fragmentation while supposing that some aspect of EONs are given.

Currently, EON is still in the research/experimental stage. The enabling technologies have been demonstrated, but they are not mature enough to be commercialized. Innovative and sophisticated devices and components must be developed in order to achieve hitless defragmentation and therefore spectrum efficient EONs. These devices must incorporate hitless retuning and lightpath reallocation capabilities to enable the presented schemes to be deployed. As the presented schemes' performances depend in part on the processing speed, efforts are to be made to improve the retuning speed and reallocation speed.

The control plane, including the synchronization during the defragmentation process, is to be addressed. The control plane is responsible for (1) the exchange of bandwidth profile information between nodes along a lightpath (2) the establishment, deletion, and allocated bandwidth modification of lightpath connections [82]. It can be centralized or decentralize [44]. As the control plane of

EONs must support many unique properties, new control protocols need to be developed or the existing protocols should be extended in order to support these unique properties [24].

Further considerations are to be taken beside the implementation of the schemes. The problems were formulated in this thesis with the assumption that parts of the implementation of an optical path, such as signaling and modulation, have already been performed. For implementation in EONs, these aspects have to be incorporated along with the network's characteristics. The defragmentation algorithms may be required to be re-adapted to take into account the network's characteristics.

With EONs enabling multiple data rates, distance adaptive modulation can be considered in parallel with hitless fragmentation to minimize the spectrum utilization. Defragmentation schemes can be developed to perform the routing, modulation and spectrum allocation in order to facilitate hitless defragmentation. For example, the use of bandwidth squeezing will allow lightpath reallocation with reduced bandwidth.

Furthermore, the work presented in this thesis can be extended to increase EON survivability with reduced backup spectrum utilization. Spectrum defragmentation can minimize the spare capacity in networks that use shared backup paths and in networks that allow bandwidth squeezed restoration [53]. This work focused on 1+1 paths protection, which is a dedicated protection where each path has its own backup. On the other hand shared backup path protection allows the reserved backup spectrum to be used for the protection of different primary paths. Bandwidth squeezed restoration allows lightpath to be restored, or reallocated, while reducing its allocated bandwidth by using a higher modulation format to the price of reduced transmission quality over the distance.

Finally, test-bed experiments are needed to confirm the performance results of the schemes presented in this thesis. The presented evaluation results are obtained through theoretical analysis and simulation. They indicate that, when implemented, the presented schemes will increase the traffic admissibility in EONs.

# 6. CONCLUSIONS AND FUTURE WORKS

# References


[1] N. G. Duffield, P. Goyal, A. Greenberg, P. Mishra, K. K. Ramakrishnan, and J. E. van der Merive, "A flexible model for resource management in virtual private networks," in *ACM SIGCOMM Computer Communication Review*, vol. 29, no. 4. ACM, 1999, pp. 95–108. 1

[2] M. Jinno, H. Takara, and B. Kozicki, "Concept and enabling technologies of spectrum-sliced elastic optical path network (slice)," in *Asia Communications and Photonics Conference and Exhibition*. Optical Society of America, 2009, p. FO2. 1

[3] M. Jinno, H. Takara, B. Kozicki, Y. Tsukishima, Y. Sone, and S. Matsuoka, "Spectrum-efficient and Scalable Elastic Optical Path Network: Architecture, Benefits, and Enabling Technologies," *IEEE Commun. Mag.*, vol. 47, no. 11, pp. 66–73, 2009. 1

[4] O. Gerstel, M. Jinno, A. Lord, and S. B. Yoo, "Elastic optical networking: A new dawn for the optical layer?" *IEEE Communications Magazine*, vol. 50, no. 2, pp. s12–s20, 2012. 1

[5] B. Kozicki, H. Takara, T. Yoshimatsu, K. Yonenaga, and M. Jinno, "Filtering characteristics of highly-spectrum efficient spectrum-sliced elastic optical path (slice) network," in *National Fiber Optic Engineers Conference*. Optical Society of America, 2009, p. JWA43. 2

[6] G. Zhang, M. De Leenheer, A. Morea, and B. Mukherjee, "A survey on ofdm-based elastic core optical networking," *IEEE Communications Surveys & Tutorials*, vol. 15, no. 1, pp. 65–87, 2013. 2

[7] M. Jinno, Y. Miyamoto, and Y. Hibino, "Networks: Optical-transport networks in 2015," *nature photonics*, vol. 1, no. 3, pp. 157–159, 2007. 2

[8] M. Jinno, H. Takara, Y. Sone, K. Yonenaga, and A. Hirano, "Multiflow optical transponder for efficient multilayer optical networking," *IEEE Communications Magazine*, vol. 50, no. 5, pp. 56–65, 2012. 3

[9] Y. Miyamoto, A. Sano, H. Masuda, E. Yoshida, and S. Aisawa, "Enhancing the capacity beyond terabit per second for transparent optical transport network," *ECOC 2007*, 2007. 3

[10] A. Sano, H. Masuda, E. Yoshida, T. Kobayashi, E. Yamada, Y. Miyamoto, F. Inuzuka, Y. Hibino, Y. Takatori, K. Hagimoto *et al.*, "30 x 100-gb/s all-optical ofdm transmission over 1300 km smf with 10 roadm nodes," *ECOC 2007*, 2007. 3

[11] T. Kobayashi, A. Sano, E. Y. Yamada, Y. Miyamoto, H. Takara, and A. Takada, "Electro-optically multiplexed 110 gbit/s optical ofdm signal transmission over 80 km smf without dispersion compensation," *Electronics Letters*, vol. 44, no. 3, p. 1, 2008. 3

[12] G. Bosco, V. Curri, A. Carena, P. Poggiolini, and F. Forghieri, "On the performance of nyquist-wdm terabit superchannels based on pm-bpsk, pm-qpsk, pm-8qam or pm-16qam subcarriers," *Journal of Lightwave Technology*, vol. 29, no. 1, pp. 53–61, 2011. 3

[13] G. Bosco, A. Carena, V. Curri, P. Poggiolini, and F. Forghieri, "Performance limits of nyquist-wdm and co-ofdm in high-speed pm-qpsk systems," *IEEE Photonics Technology Letters*, vol. 22, no. 15, pp. 1129–1131, 2010. 3

[14] T. Tanaka, A. Hirano, and M. Jinno, "Impact of transponder architecture on the scalability of optical nodes in elastic optical networks," *IEEE Communications Letters*, vol. 17, no. 9, pp. 1846–1848, 2013. 3

[15] N. Sambo, P. Castoldi, A. D'Errico, E. Riccardi, A. Pagano, M. S. Moreolo, J. M. Fàbrega, D. Rafique, A. Napoli, S. Frigerio *et al.*, "Next generation

sliceable bandwidth variable transponders," *IEEE Communications Magazine*, vol. 53, no. 2, pp. 163–171, 2015. 3

[16] S. Frisken, G. Baxter, D. Abakoumov, H. Zhou, I. Clarke, and S. Poole, "Flexible and grid-less wavelength selective switch using lcos technology," in *Optical Fiber Communication Conference*. Optical Society of America, 2011, p. OTuM3. 4

[17] R. Ryf, Y. Su, L. Moller, S. Chandrasekhar, X. Liu, D. T. Neilson, and C. R. Giles, "Wavelength blocking filter with flexible data rates and channel spacing," *Journal of lightwave technology*, vol. 23, no. 1, pp. 54–61, 2005. 4

[18] G. Baxter, S. Frisken, D. Abakoumov, H. Zhou, I. Clarke, A. Bartos, and S. Poole, "Highly programmable wavelength selective switch based on liquid crystal on silicon switching elements," in *Optical Fiber Communication Conference*. Optical Society of America, 2006, p. OTuF2. 4

[19] M. Jinno, T. Ohara, Y. Sone, A. Hirano, O. Ishida, and M. Tomizawa, "Introducing elasticity and adaptation into the optical domain toward more efficient and scalable optical transport networks," in *Kaleidoscope: Beyond the Internet?-Innovations for Future Networks and Services, 2010 ITU-T*. IEEE, 2010, pp. 1–7. 4

[20] E. Kosmatos, T. Orphanoudakis, C. Matrakidis, A. Stavdas, and A. Lord, "Switchless elastic rate node (serano) architecture: A universal node for optical grooming and adaptive networking," *Journal of Optical Communications and Networking*, vol. 8, no. 7, pp. A162–A170, 2016. 4

[21] K. Christodoulopoulos, I. Tomkos, and E. A. Varvarigos, "Routing and spectrum allocation in ofdm-based optical networks with elastic bandwidth allocation," in *Global Telecommunications Conference (GLOBECOM 2010), 2010 IEEE*. IEEE, 2010, pp. 1–6. 4

[22] Y. Wang, X. Cao, and Y. Pan, "A Study of the Routing and Spectrum Allocation in Spectrum-Sliced Elastic Optical Path Networks," in *Proc. IEEE Infocom*. IEEE, Apr. 2011, pp. 1503–1511. 4

[23] Y. Wang, X. Cao, and Q. Hu, "Routing and spectrum allocation in spectrum-sliced elastic optical path networks," in *2011 IEEE International Conference on Communications (ICC)*. IEEE, 2011, pp. 1–5. 4

[24] B. C. Chatterjee, N. Sarma, and E. Oki, "Routing and spectrum allocation in elastic optical networks: a tutorial," *IEEE Communications Surveys & Tutorials*, vol. 17, no. 3, pp. 1776–1800, 2015. 4, 91

[25] C.-F. Hsu, Y.-C. Chang, and S.-C. Sie, "Graph-model-based dynamic routing and spectrum assignment in elastic optical networks," *Journal of Optical Communications and Networking*, vol. 8, no. 7, pp. 507–520, 2016. 4

[26] B. Kozicki, H. Takara, A. Watanabe, Y. Sone, T. Tanaka, A. Hirano, K. Yonenaga, and M. Jinno, "Distance-adaptive spectrum allocation in slice considering optical filtering effects," in *OECC 2010 Technical Digest*, 2010. 5

[27] M. Jinno, B. Kozicki, H. Takara, A. Watanabe, Y. Sone, T. Tanaka, and A. Hirano, "Distance-adaptive Spectrum Resource Allocation in Spectrum-sliced Elastic Optical Path Network (Topics in Optical Communications)," *IEEE Commun. Mag.*, vol. 48, no. 8, pp. 138–145, 2010. 5

[28] M. Jinno and H. Takara, "Elastic optical transponder and regenerator: Toward energy and spectrum efficient optical transport networks," in *2012 International Conference on Photonics in Switching (PS)*, Sept 2012, pp. 1–3. 5

[29] S. Yang and F. Kuipers, "Impairment-aware routing in translucent spectrum-sliced elastic optical path networks," in *Networks and Optical Communications (NOC), 2012 17th European Conference on*. IEEE, 2012, pp. 1–6. 5

[30] H. Beyranvand and J. A. Salehi, "A quality-of-transmission aware dynamic routing and spectrum assignment scheme for future elastic optical networks," *Journal of Lightwave Technology*, vol. 31, no. 18, pp. 3043–3054, 2013. 5

[31] M. Klinkowski, "On the effect of regenerator placement on spectrum usage in translucent elastic optical networks," in *2012 14th International Conference on Transparent Optical Networks (ICTON)*. IEEE, 2012, pp. 1–6. 5

[32] W. Shi, Z. Zhu, M. Zhang, and N. Ansari, "On the Effect of Bandwidth Fragmentation on Blocking Probability in Elastic Optical Networks," *IEEE Trans. on Commun.*, vol. 61, no. 7, pp. 2970–2978, 2013. 6

[33] J. Kim, S. Yan, A. Fumagalli, E. Oki, and N. Yamanaka, "An analytical model of spectrum fragmentation in a two-service elastic optical link," in *2015 IEEE Global Communications Conference (GLOBECOM)*. IEEE, 2015, pp. 1–6. 6

[34] Y. Yin, H. Zhang, M. Zhang, M. Xia, Z. Zhu, S. Dahlfort, and S. B. Yoo, "Spectral and spatial 2d fragmentation-aware routing and spectrum assignment algorithms in elastic optical networks [invited]," *Journal of Optical Communications and Networking*, vol. 5, no. 10, pp. A100–A106, 2013. 6

[35] X. Chen, J. Li, P. Zhu, R. Tang, Z. Chen, and Y. He, "Fragmentation-aware routing and spectrum allocation scheme based on distribution of traffic bandwidth in elastic optical networks," *Journal of Optical Communications and Networking*, vol. 7, no. 11, pp. 1064–1074, 2015. 6

[36] R. Wang and B. Mukherjee, "Spectrum management in heterogeneous bandwidth networks," in *Global Communications Conference (GLOBECOM), 2012 IEEE*. IEEE, 2012, pp. 2907–2911. 6

[37] W. Fadini and E. Oki, "A Subcarrier-slot Partition Scheme for Wavelength Assignment in Elastic Optical Networks," in *IEEE International Conference on High Performance Switching and Routing (HPSR)*. IEEE, July 2014, pp. 7–12. 7

[38] W. Fadini, B. C. Chatterjee, and E. Oki, "A subcarrier-slot partition scheme with first-last fit spectrum allocation for elastic optical networks," *Computer Networks*, vol. 91, pp. 700–711, 2015. 7

[39] M. Zhang, W. Shi, L. Gong, W. Lu, and Z. Zhu, "Bandwidth Defragmentation in Dynamic Elastic Optical Networks with Minimum Traffic Disruptions," in *IEEE International Conference on Communications (ICC)*. IEEE, June 2013, pp. 3894–3898. 7

[40] M. Zhang, C. You, H. Jiang, and Z. Zhu, "Dynamic and Adaptive Bandwidth Defragmentation in Spectrum-Sliced Elastic Optical Networks With Time-Varying Traffic," *J. of Lightwave Technol.*, vol. 32, no. 5, pp. 1014–1023, 2014. 7

[41] X. Chen, A. Jukan, and A. Gumaste, "Multipath de-fragmentation: Achieving better spectral efficiency in elastic optical path networks," in *INFOCOM, 2013 Proceedings IEEE*. IEEE, 2013, pp. 390–394. 7

[42] A. Pagès, J. Perelló, S. Spadaro, J. Comellas *et al.*, "Optimal route, spectrum, and modulation level assignment in split-spectrum-enabled dynamic elastic optical networks," *Journal of Optical Communications and Networking*, vol. 6, no. 2, pp. 114–126, 2014. 7

[43] P. Zhu, J. Li, D. Wu, Z. Wu, Y. Tian, Y. Chen, D. Ge, X. Chen, Z. Chen, and Y. He, "Demonstration of elastic optical network node with defragmentation functionality and sdn control," in *Optical Fiber Communication Conference*. Optical Society of America, 2016, pp. Th3I–3. 7

[44] X. Wang, I. Kim, Q. Zhang, P. Palacharla, and M. Sekiya, "A hitless defragmentation method for self-optimizing flexible grid optical networks," in *European Conference and Exhibition on Optical Communication*. Optical Society of America, 2012, pp. P5–04. 8, 90

[45] R. Proietti, C. Qin, B. Guan, Y. Yin, R. P. Scott, R. Yu, and S. Yoo, "Rapid and complete hitless defragmentation method using a coherent rx lo with fast wavelength tracking in elastic optical networks," *Optics express*, vol. 20, no. 24, pp. 26 958–26 968, 2012. 8, 9

[46] Y. Aoki, X. Wang, P. Palacharla, K. Sone, S. Oda, T. Hoshida, M. Sekiya, and J. C. Rasmussen, "Dynamic and flexible photonic node architecture

with shared universal transceivers supporting hitless defragmentation," in *European Conference and Exhibition on Optical Communication*. Optical Society of America, 2012, pp. We–3. 8, 10, 11, 12, 22, 82

[47] M. Zhang, Y. Yin, R. Proietti, Z. Zhu, and S. Yoo, "Spectrum defragmentation algorithms for elastic optical networks using hitless spectrum retuning techniques," in *Optical Fiber Communication Conference*. Optical Society of America, 2013, pp. OW3A–4. 9

[48] F. Cugini, F. Paolucci, G. Meloni, G. Berrettini, M. Secondini, F. Fresi, N. Sambo, L. Poti, and P. Castoldi, "Push-pull defragmentation without traffic disruption in flexible grid optical networks," *Lightwave Technology, Journal of*, vol. 31, no. 1, pp. 125–133, 2013. 10

[49] R. Muñoz, R. Casellas, R. Martínez, L. Liu, T. Tsuritani, and I. Morita, "Experimental evaluation of efficient routing and distributed spectrum allocation algorithms for gmpls elastic networks," *Optics express*, vol. 20, no. 27, pp. 28 532–28 537, 2012. 11

[50] S. Ma, C. Chen, S. Li, M. Zhang, S. Li, Y. Shao, Z. Zhu, L. Liu, and S. B. Yoo, "Demonstration of online spectrum defragmentation enabled by openflow in software-defined elastic optical networks," in *OFC 2014*, 2014, pp. 1–3. 11

[51] M. Sekiya, W. Xi, Y. Aoki, and K. Sone, "Photonic network defragmentation technology improving resource utilization during operation," *FUJITSU Sci. Tech. J*, vol. 50, no. 1, pp. 101–109, 2014. 12, 14, 37

[52] R. Wang and B. Mukherjee, "Provisioning in elastic optical networks with non-disruptive defragmentation," *Journal of Lightwave Technology*, vol. 31, no. 15, pp. 2491–2500, 2013. 12

[53] G. Shen, H. Guo, and S. K. Bose, "Survivable elastic optical networks: survey and perspective," *Photonic Network Communications*, vol. 31, no. 1, pp. 71–87, 2016. 12, 14, 91

[54] R. Goścień, K. Walkowiak, and M. Tornatore, "Survivable multipath routing of anycast and unicast traffic in elastic optical networks," *Journal of Optical Communications and Networking*, vol. 8, no. 6, pp. 343–355, 2016. 12

[55] C. Wang, G. Shen, B. Chen, and L. Peng, "Protection path-based hitless spectrum defragmentation in elastic optical networks: shared backup path protection," in *Optical Fiber Communications Conference and Exhibition (OFC), 2015*. IEEE, 2015, pp. 1–3. 12

[56] Y. Wei, G. Shen, and S. K. Bose, "Span-restorable elastic optical networks under different spectrum conversion capabilities," *Reliability, IEEE Transactions on*, vol. 63, no. 2, pp. 401–411, 2014. 12, 13

[57] Y. Wei, K. Xu, H. Zhao, and G. Shen, "Applying p-cycle technique to elastic optical networks," in *Optical Network Design and Modeling, 2014 International Conference on*. IEEE, 2014, pp. 1–6. 13

[58] Y. Sone, A. Watanabe, W. Imajuku, Y. Tsukishima, B. Kozicki, H. Takara, and M. Jinno, "Bandwidth squeezed restoration in spectrum-sliced elastic optical path networks (slice)," *Journal of Optical Communications and Networking*, vol. 3, no. 3, pp. 223–233, 2011. 13

[59] H. M. Oliveira and N. L. Da Fonseca, "Protection in elastic optical networks against up to two failures based fipp p-cycle," in *Computer Networks and Distributed Systems (SBRC), 2014 Brazilian Symposium on*. IEEE, 2014, pp. 369–375. 13

[60] S. Kosaka, H. Hasegawa, K.-i. Sato, T. Tanaka, A. Hirano, and M. Jinno, "Shared protected elastic optical path network design that applies iterative re-optimization based on resource utilization efficiency measures," in *European Conference and Exhibition on Optical Communication*. Optical Society of America, 2012, pp. Tu–4. 13

[61] K. Walkowiak and M. Klinkowski, "Shared backup path protection in elastic optical networks: Modeling and optimization," in *Design of Reliable Communication Networks (DRCN), 2013 9th International Conference on the*. IEEE, 2013, pp. 187–194. 13

[62] A. Tarhan and C. Cavdar, "Shared path protection for distance adaptive elastic optical networks under dynamic traffic," in *Ultra Modern Telecommunications and Control Systems and Workshops (ICUMT), 2013 5th International Congress on.* IEEE, 2013, pp. 62–67. 13

[63] X. Shao, Y.-K. Yeo, Z. Xu, X. Cheng, and L. Zhou, "Shared-path protection in ofdm-based optical networks with elastic bandwidth allocation," in *Optical Fiber Communication Conference.* Optical Society of America, 2012, pp. OTh4B–4. 13

[64] M. Klinkowski, "An evolutionary algorithm approach for dedicated path protection problem in elastic optical networks," *Cybernetics and Systems*, vol. 44, no. 6-7, pp. 589–605, 2013. 13

[65] C. Wang, G. Shen, and L. Peng, "Protection path-based hitless spectrum defragmentation for elastic optical networks: 1+ 1 path protection," in *Asia Communications and Photonics Conference.* Optical Society of America, 2014, pp. AF3E–3. 13, 14, 54, 78, 82

[66] E. Oki, *Linear Programming and Algorithms for Communication Networks.* CRC Press, 2013. 27, 76

[67] F. Barahona and A. R. Mahjoub, "On the cut polytope," *Mathematical programming*, vol. 36, no. 2, pp. 157–173, 1986. 27

[68] R. M. Karp, *Reducibility among combinatorial problems.* Springer, 1972. 28, 35

[69] I. Chlamtac, A. Ganz, and G. Karmi, "Lightpath communications: An approach to high bandwidth optical wan's," *Communications, IEEE Transactions on*, vol. 40, no. 7, pp. 1171–1182, 1992. 29, 65

[70] S. Baroni and P. Bayvel, "Wavelength requirements in arbitrarily connected wavelength-routed optical networks," *Lightwave Technology, Journal of*, vol. 15, no. 2, pp. 242–251, 1997. 34

[71] S. Sahni and T. Gonzalez, "P-complete approximation problems," *Journal of the ACM (JACM)*, vol. 23, no. 3, pp. 555–565, 1976. 35

[72] M. X. Goemans and D. P. Williamson, "Improved approximation algorithms for maximum cut and satisfiability problems using semidefinite programming," *Journal of the ACM (JACM)*, vol. 42, no. 6, pp. 1115–1145, 1995. 36

[73] B. Mukherjee, *Optical WDM networks.* Springer Science & Business Media, 2006. 37, 79

[74] IBM ILOG CPLEX 12.6, 2013. 38, 78

[75] B. Borchers, "Csdp, a c library for semidefinite programming," *Optimization methods and Software*, vol. 11, no. 1-4, pp. 613–623, 1999. 38

[76] N. Kawase, Y. Yamabayashi, M. Tomizawa, and Y. Uematsu, "Route diversity with hitless path switching," *Electronics letters*, vol. 30, no. 23, pp. 1962–1963, 1994. 51

[77] N. Kawase, Y. Yamabayashi, and Y. Uematsu, "Hitless path switching apparatus and method," May 20 1997, uS Patent 5,631,896. [Online]. Available: http://www.google.com/patents/US5631896 51

[78] H. Ueda, T. Tsuboi, and H. Kasai, "Hitless switching scheme for protected pon system," in *Global Telecommunications Conference, 2008. IEEE GLOBECOM 2008. IEEE.* IEEE, 2008, pp. 1–5. 51

[79] A. Lodi, S. Martello, and D. Vigo, "Recent advances on two-dimensional bin packing problems," *Discrete Applied Mathematics*, vol. 123, no. 1, pp. 379–396, 2002. 58, 71, 72

[80] B. S. Baker, E. G. Coffman, Jr, and R. L. Rivest, "Orthogonal packings in two dimensions," *SIAM Journal on Computing*, vol. 9, no. 4, pp. 846–855, 1980. 71, 72

[81] J. O. Berkey and P. Y. Wang, "Two-dimensional finite bin-packing algorithms," *Journal of the operational research society*, vol. 38, no. 5, pp. 423–429, 1987. 71, 72

[82] Y. Sone, A. Watanabe, W. Imajuku, Y. Tsukishima, B. Kozicki, H. Takara, and M. Jinno, "Highly survivable restoration scheme employing optical bandwidth squeezing in spectrum-sliced elastic optical path (slice) network," in *Optical Fiber Communication Conference*. Optical Society of America, 2009, p. OThO2. 90

# Publications

## List of Publications Related to Thesis

### Journal Papers

1. S. Ba, B. C. Chatterjee, S. Okamoto, N. Yamanaka, A. Fumagalli, and E. Oki, "Route Partitioning Scheme for Elastic Optical Networks with Hitless Defragmentation," IEEE/OSA J. Opt. Commun. Netw., vol. 8, no. 6, pp. 356-370, 2016.

2. S. Ba, B. C. Chatterjee, and E. Oki, "Defragmentation Scheme Based on Exchanging Primary and Backup Paths in 1+1 Path Protected Elastic Optical Networks", IEEE/ACM Transactions on Networking (In press).

### International Conference Papers

1. S. Ba, B. C. Chatterjee, and E. Oki, "Performance of Route Partitioning Scheme for Hitless Defragmentation in Elastic Optical Networks," International Conference on Computing, Networking and Communications (ICNC) Jan. 2017 .

## List of Other Publications

### Journal Papers

1. S. Ba, I. A. Ouédraogo , and E. Oki, "Reducing the Power Consumption of Hose-Model Networks with Bundled Links," IET Networks, Vol. 4, no.2,

pp: 119-127, 2015.

## International Conference Papers

1. S. Ba, B. C. Chatterjee, A. Kawabata, and E. Oki, "Computational Time Complexity of Allocation Problem for Distributed Servers in Real-time Applications", The Asia-Pacific Network Operations and Management Symposium (APNOMS), Oct. 2016.

2. S. Ba, I. A. Ouédraogo , and E. Oki, "A Power Consumption Reduction Scheme in Hose-Model Networks with Bundled Links," Green Computing and Communications (GreenCom), 2013 IEEE and Internet of Things (iThings/CPSCom), IEEE International Conference on and IEEE Cyber, Physical and Social Computing, pp.40,45, 20-23 Aug. 2013.

## National Conference Papers

1. S. Ba, I. A. Ouédraogo , and E. Oki, "Performance of Energy Efficient Network Resource Allocation Scheme for Hose Model," IEICE technical report (NS), Mar. 2014.

2. Y. Kishi, S. Ba, and E. Oki, "Spectrum Slot Defragmentation in Elastic Optical Networks," IEICE Student Branch, Tokyo, Mar. 2016.